

Phylis Makurunje¹, Fabio Martini¹, Sarah Valley¹, Alberto Fraile¹, Dave Goddard², Nicholas Barron², James Gath², Simon Middleburgh¹

¹ Nuclear Futures Institute, Bangor University, Bangor, Gwynedd, LL57 1UT, United Kingdom
² National Nuclear Laboratory, Preston Laboratory, Springfields, Preston, Lancashire PR4 0XJ, United Kingdom

Introduction

State-of-the-art composite nuclear fuels for improved reactor operational efficiency and accident tolerance are largely made of ceramic kernel-ceramic matrix fuel combinations.

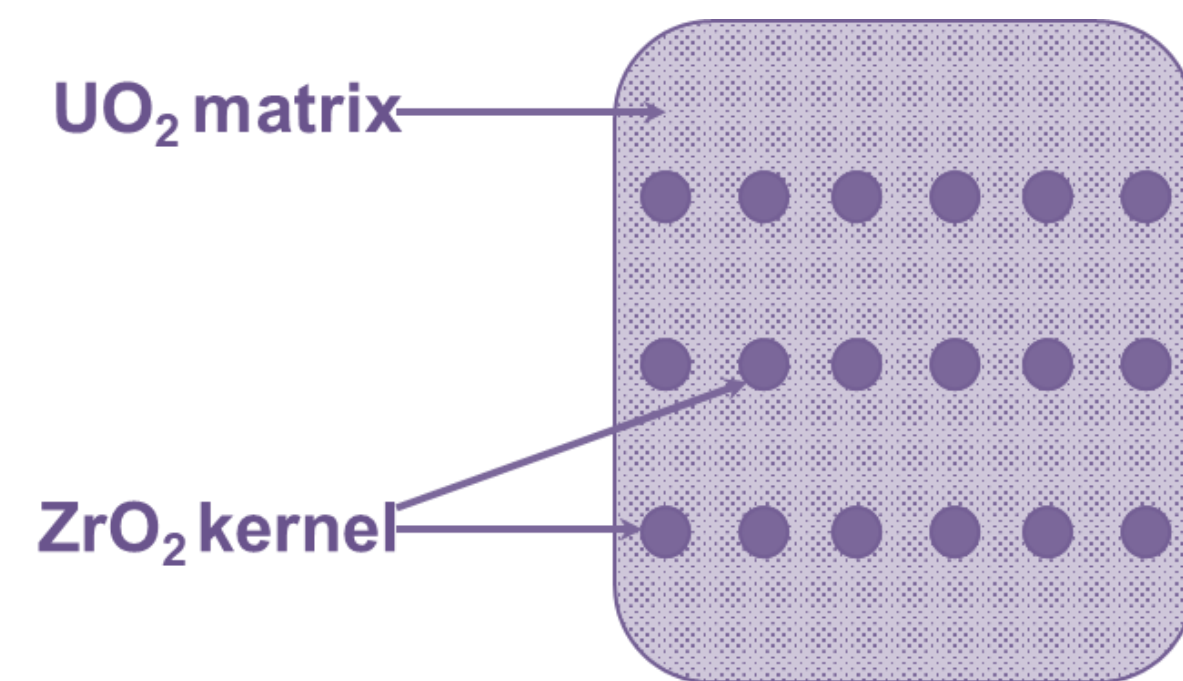
Such composite fuels must possess the following characteristics [1]:

- Higher thermal conductivity than current (uranium dioxide) fuels
- Improved reaction kinetics with steam to minimise enthalpy input and hydrogen generation
- The ability to contain volatile fission products
- The ability to resist high temperature oxidation and/or form a protective oxide layer

Composite fuels typically consist of solid, dense kernels that are dispersed in a UO₂-matrix, pressed into pellets and sintered.

Different ceramic combinations are possible – fissile or non-fissile kernels in a matrix which can also be fissile or non-fissile.

Our work has covered ZrB₂ [2] and ZrN [3] ceramics dispersed in UO₂. Now, we demonstrate ZrO₂, as an oxide ceramic option.



Ceramic kernels can be manufactured by sol-gel or granulation techniques. This work has focused on gel casting, a wet granulation technique for near net shape formation of kernels.

After successfully demonstrating the spray drying process [4], to manufacture kilograms of kernels per minute, we demonstrate a gel casting process for the manufacture of composite fuels.

Objectives

This project sought to provide a route for the manufacture of a composite fuel consisting of ZrO₂-kernels dispersed in a UO₂-matrix.

1. Manufacture kernels by gel-casting (wet granulation) route
2. Compare with kernels manufactured by spray drying (wet granulation)
3. Compare the ZrO₂/UO₂ composite fuel prepared (ZrO₂-kernels dispersed in a UO₂-matrix)

Materials and Methods

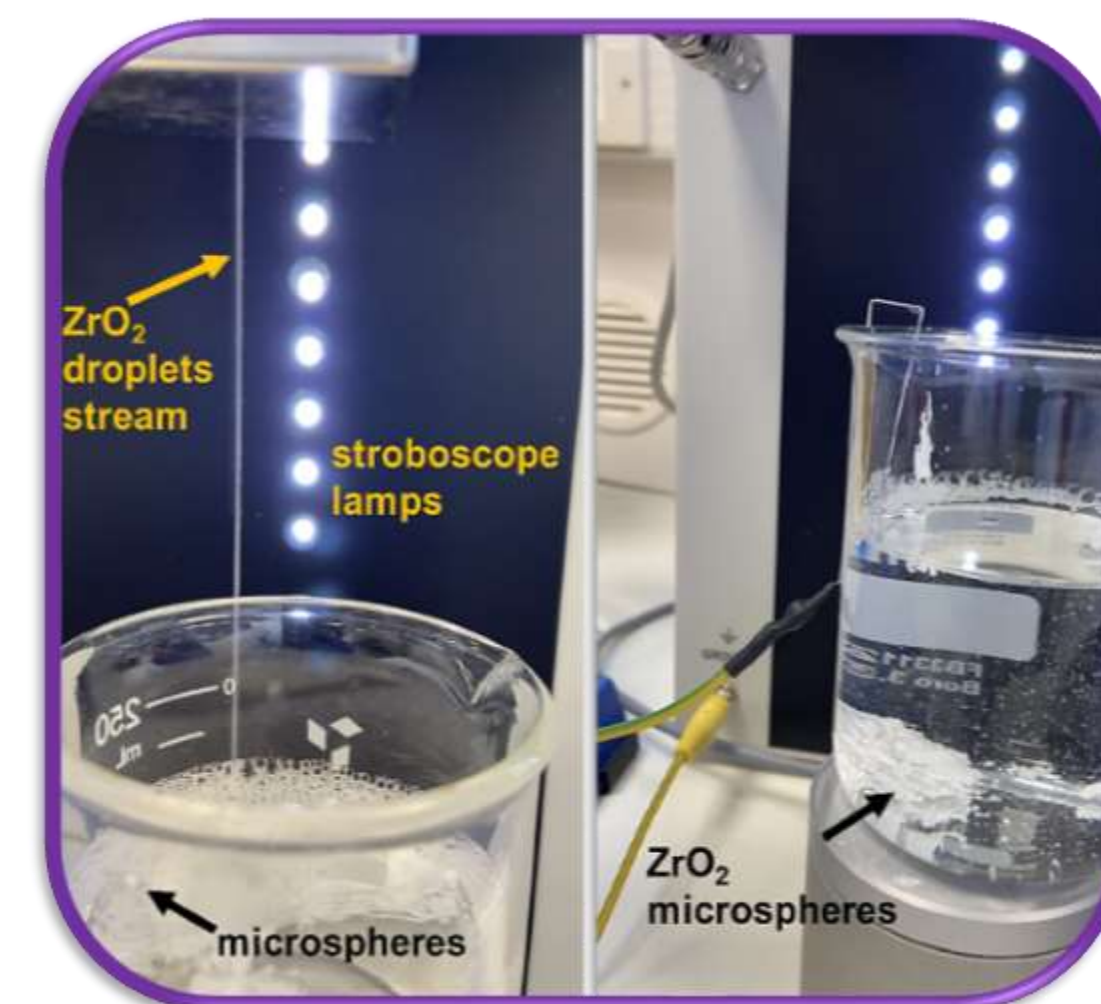
A zirconium oxide slurry was modified by an alginate polymer matrix together with binder and dispersant surfactants.

The granulation nozzle was vibrated in the range of 0.25-3 kHz for the 70 wt% surrogate powder loaded slurry to produce spherical droplets.

Droplets solidified into kernels upon contact with a 1M calcium solution.

Kernels were dispersed into UO₂ powders, compacted into pellets and sintered at 1700 °C for 2 h in 5%hydrogen-argon atmosphere.

Results



Spray dried kernels

Gel cast kernels

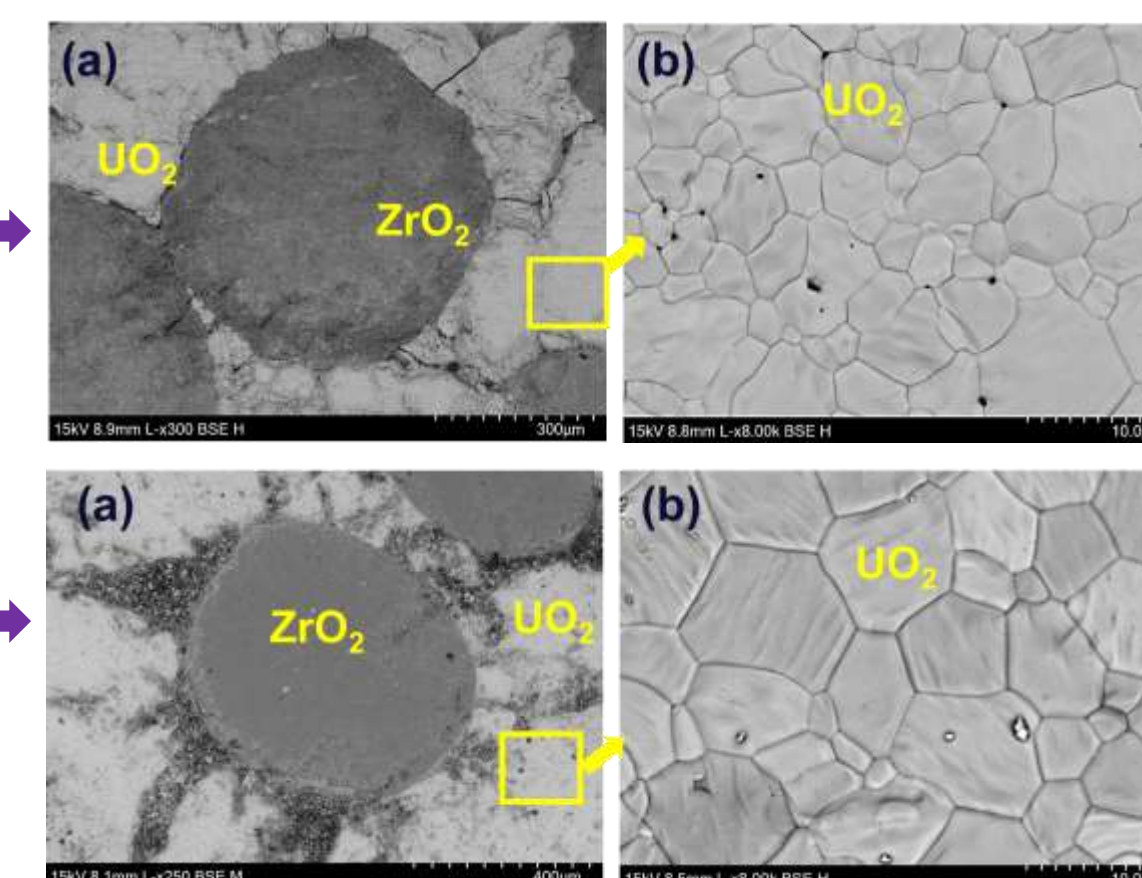


Figure 3: Encapsulated ZrO₂ dispersed in UO₂ matrix.



Figure 3: Gel casting equipment used to produce ZrO₂ kernels (Source: Buchi)

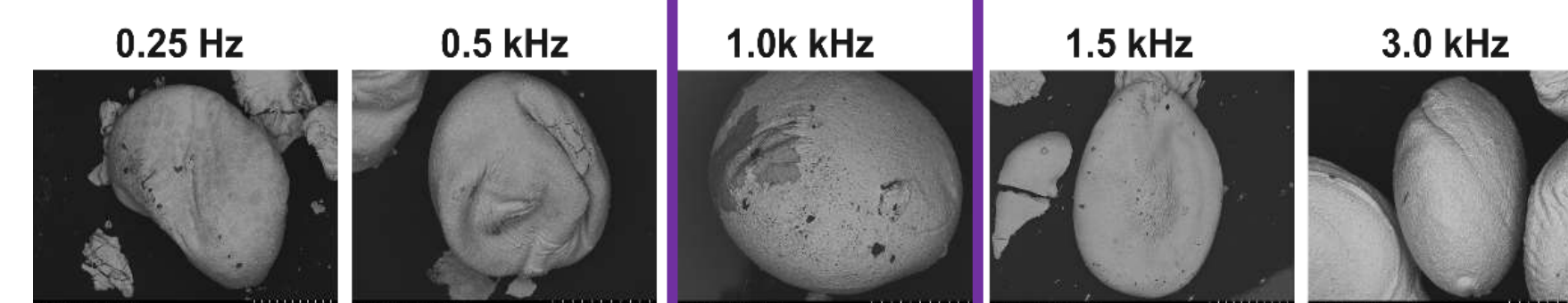


Figure 1: Kernels produced by varying the nozzle vibration in the range of 0.25-3kHz (Slurry feed rate = 10 ml/min).

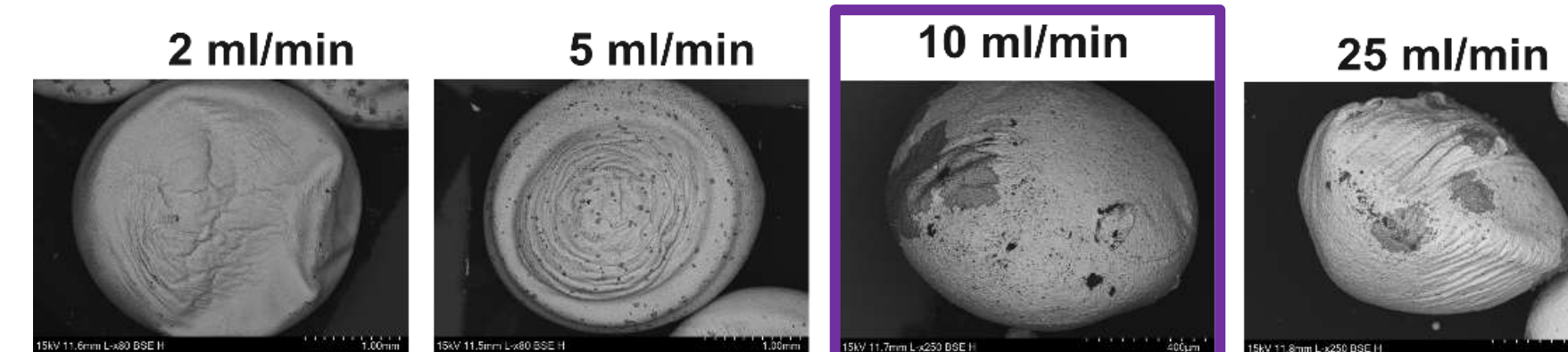


Figure 2: Kernels produced by varying the slurry feed rate to the nozzle in the range of 2-25 ml/min (vibration = 1kHz). The kernel diameter decreased with increased feed rate.

Conclusions

A composite fuel consisting of ZrO₂-kernels dispersed in a UO₂-matrix was successfully prepared.

ZrO₂-kernels manufactured by gel-casting, a wet granulation technique, were obtained.

Optimisation of the gel-casting method involved adjusting the casting nozzle vibration frequency and the ZrO₂ slurry feed rate.

Optimal parameters for producing ~200-500 µm diameter kernels were 10 mL/min feed and 1 kHz nozzle vibration.

Composite fuel pellets produced will be exposed to Xe ions to study radiation damage effects.

Current gel casting and spray drying work is focusing on manufacturing on uranium dioxide kernels

Future work will look at coating the kernels (to produce TRISO particles as used in HTGRs) and performing the gel casting method on other uranium ceramic kernels for composite fuels.

References

1. K.A. Terrani. *Accident tolerant fuel cladding development: Promise, status, and challenges*. Journal of Nuclear Materials, 501, 13-30 (2018).
2. P. Makurunje et al. *Gel cast zirconium diboride kernels for surrogate and neutron absorbing kernels in composite nuclear fuels*. To be submitted to Journal of Nuclear Materials (2022)
3. D.R. Costa et al. *Fabrication and characterisation of coated ZrN spheres-UO₂ composites as surrogates for UN-UO₂ accident tolerant fuels*, submitted to Journal of Nuclear Materials (2022)
4. P. Makurunje et al. *Self-contained dual-scale composite architectures in spray dried zirconium diboride*. Ceramics International, in press. (2022)

Acknowledgements

This research was funded under the £46m Advanced Fuel Cycle Programme as part of the Department for Business, Energy and Industrial Strategy's (BEIS) £505m Energy Innovation Programme.

Contact

Phylis Makurunje - p.makurunje@bangor.ac.uk
Simon Middleburgh - s.middleburgh@bangor.ac.uk

The mechanism of the kernel granulation was observed as consisting of slurry sheet fusion, rapid deformation (folding and spheroidization) and solidification via ion exchange within the alginate polymer matrix.

Kernels were in the range of ~200-500µm diameter after sintering.

Spray dried kernels were more spherical; gel cast spheres were denser.

The composite fuel produced had 38.6 vol% (20 wt%) of ZrO₂ in UO₂.

Pellets were 10 mm diameter, 6 mm in height and showed densely sintered microstructures.

1. Time Domain Thermoreflectance (TDTR)

A near-surface optical technique that exploits the relationship between *temperature* and *reflectance*. A change in **reflectance** intensity is proportional to a change in **temperature** and is used to calculate cross-sectional thermal conductivity using transmission line theory.

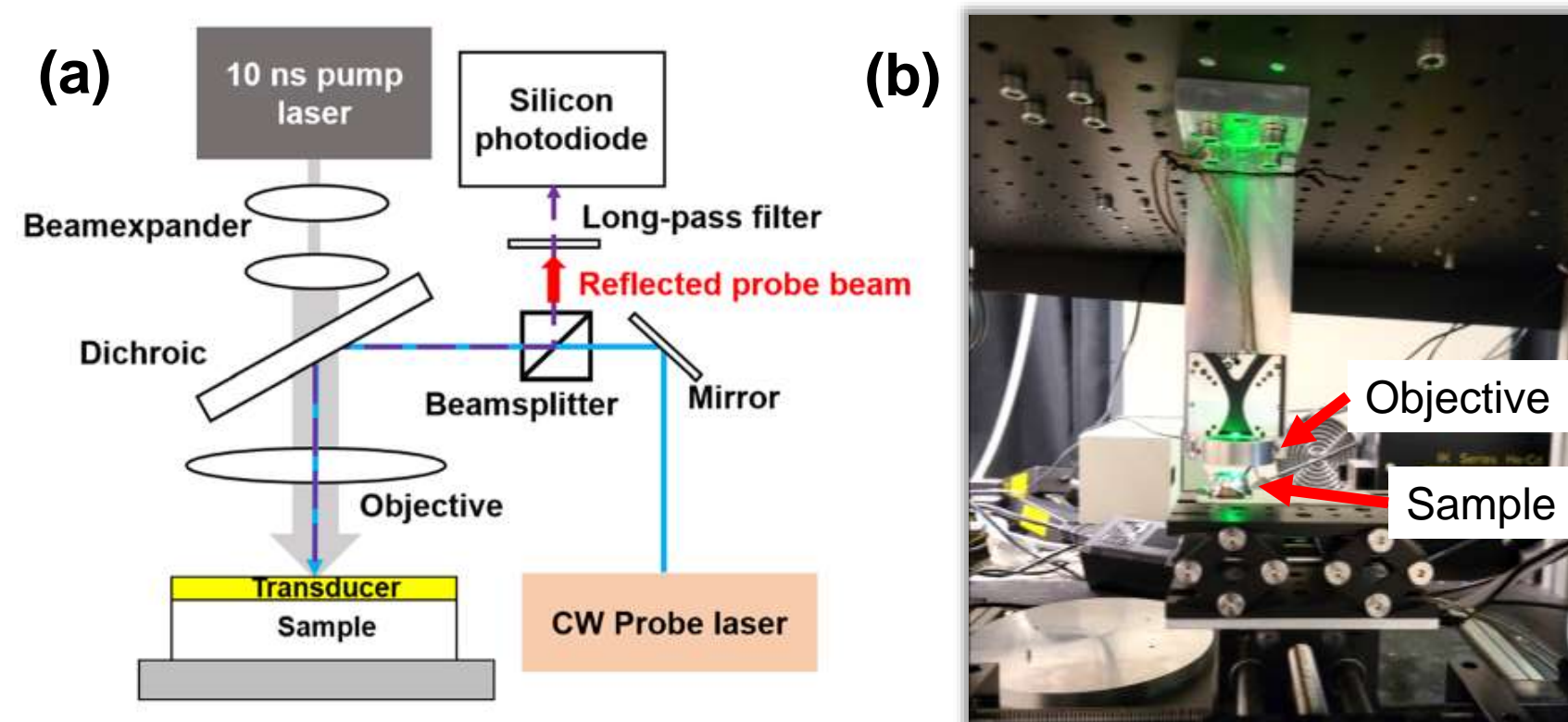
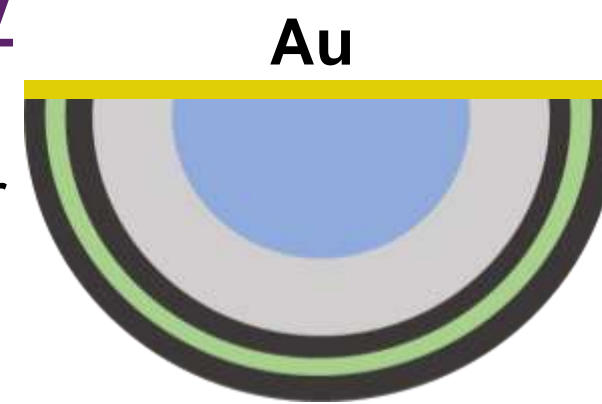


Fig. 1 (a) Schematic of TDTR setup. (b) Picture of sample on optical stage

2. Cross-Sectional Thermal Conductivity

A cross-section of a surrogate TRISO particle in a SiC matrix was coated with 150 nm Au transducer and a 10 nm Cr adhesion layer by thermal evaporation to normalize the thermoreflectance.



Two sets of measurements have been taken for the three layers. The PyC layers were fitted using a thermal conductivity value of HOPG, 10.5 ± 2 W/m·K, which was determined using the TDTR set up. The SiC layer was fitted using the value from Lopez-Honorato et al. [1], 168 W/m·K.

Table 1: Thermal conductivity for each layer in the measurement sets

Measurement Set	Layer	Thermal Conductivity (W/m·K)	Standard Deviation
Set 1	IPyC	22.53	±1
	OPyC	18.67	±9
	SiC	151.00	±14
Set 2	IPyC	23.77	±5
	OPyC	18.69	±5
	SiC	169.50	±33

3. Cross-Sectional Thermal Conductivity Traces

Typical traces are shown for the cross-sectional thermal conductivity measurements shown in 'Table 1'. A radial line-scan across the different layers was undertaken demonstrating a **reduced thermal conductivity** in SiC layer towards the OPyC boundary, and **lower conductivity of OPyC**.

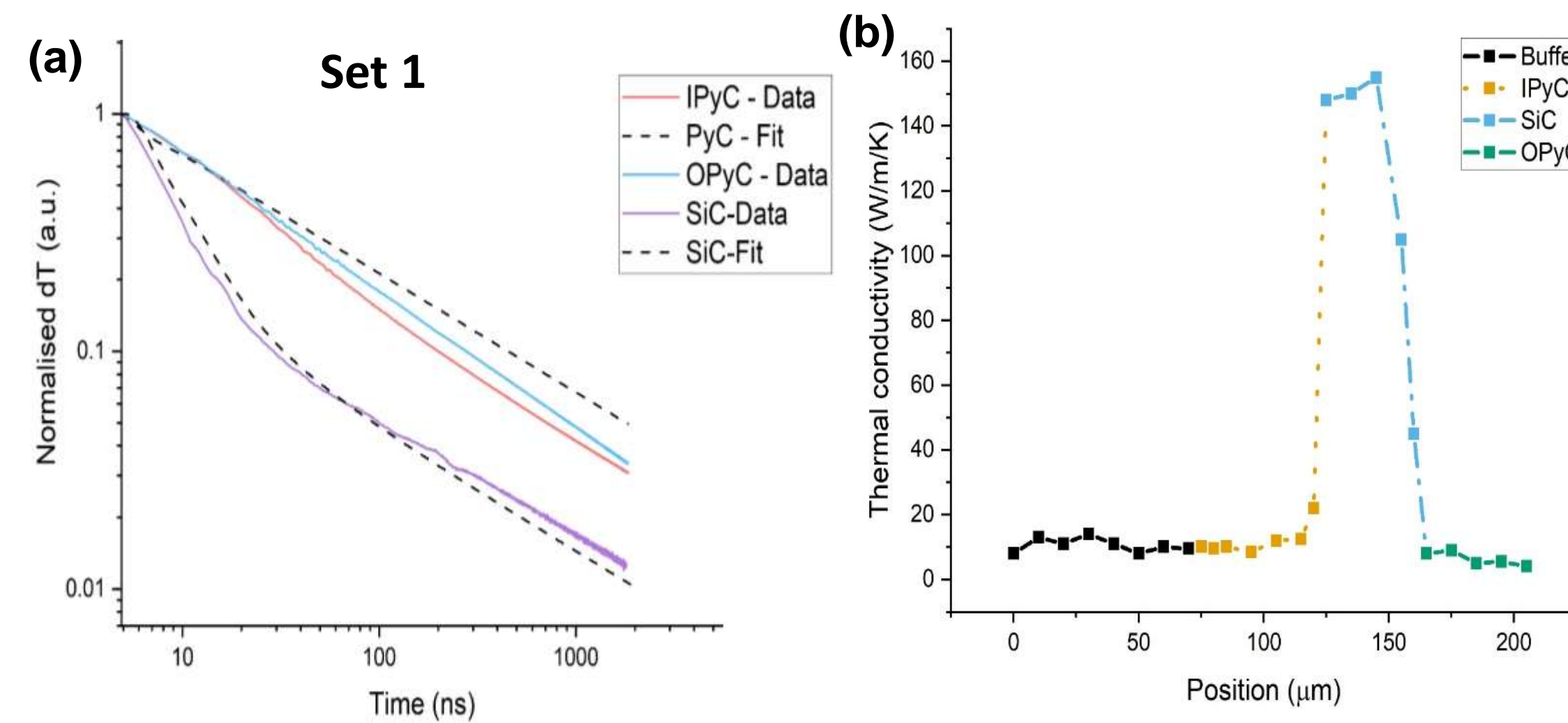


Fig. 2 (a) A typical set of TDTR trace fitting used for calculating thermal conductivity; (b) thermal conductivity data taken in a radial line-scan across the four TRISO layers.

4. SiC-OPyC Boundary Effect

Based on 3D FEM and thermoreflectance simulations to assess the resolution of this method, experimental results should not be affected by the OPyC boundary until ~ 5 μm away. This suggests that lower outer SiC thermal conductivity is real.

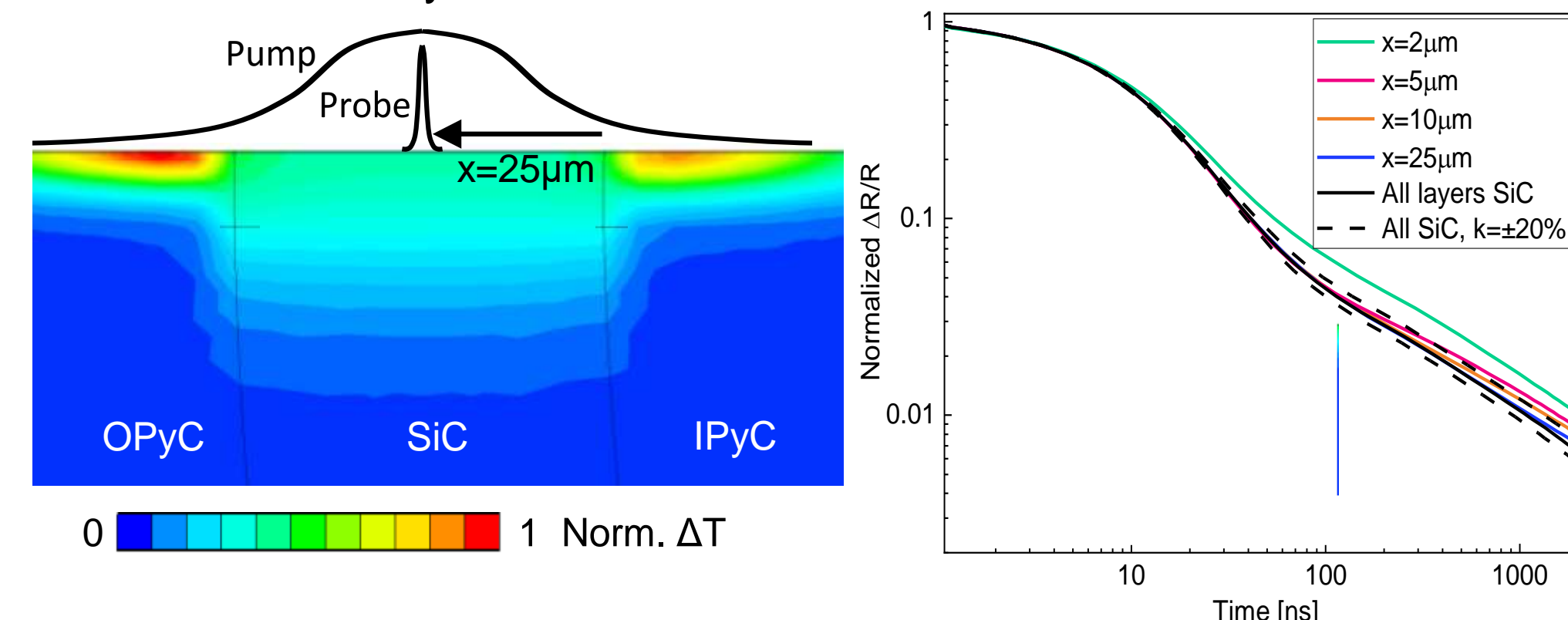


Fig. 3 Finite element modelling of laser induced change in temperature distribution

5. Temperature Profile Simulations

3D Finite Element Modelling of temperature profile in idealized TRISO.

- Complete, intact TRISO
- Irradiated TRISO with buffer shrinkage and gas gap.

Negligible temperature-drop through dense coatings.

Gas gaps/debonding is **highly significant**.

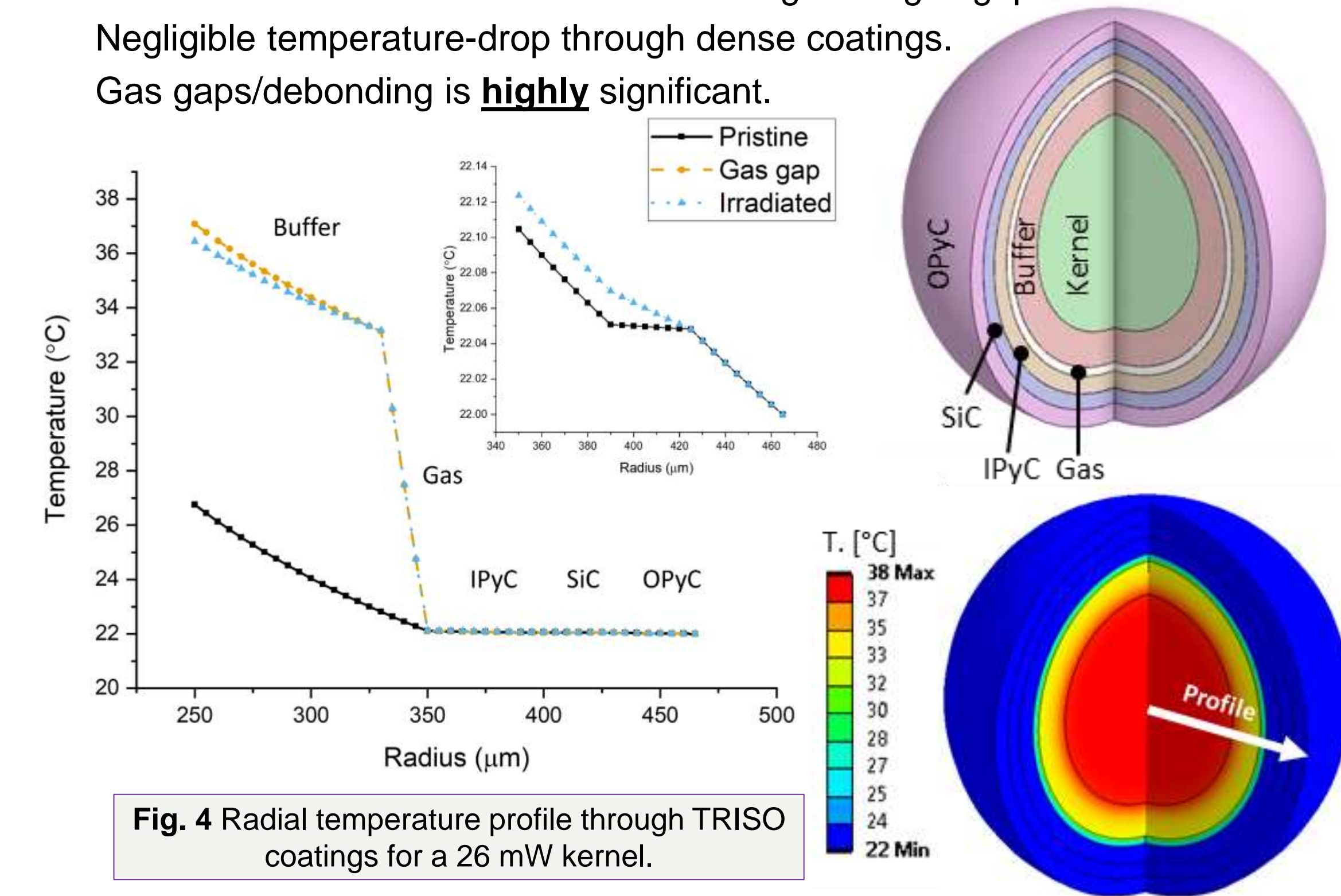


Fig. 4 Radial temperature profile through TRISO coatings for a 26 mW kernel.

6. Conclusions

- Results are self consistent, further measurements on standard bulk SiC would complete calibration.
- The data follow trends seen in literature, e.g. *IPyC* having a higher thermal conductivity than OPyC, and SiC having a lower thermal conductivity than assumed.
- TDTR is a promising near surface technique to determine **local thermal conductivity** of various nuclear materials.

7. References, Acknowledgements & Contacts

[1] López-Honorato et al. (2008), J. Nucl. Mater. 378 (2008) 35–39.

This work was funded under the £46m Advanced Fuel Cycle Programme as part of the Department for Business, Energy and Industrial Strategy's (BEIS) £505m Energy Innovation Programme.

Thanks to **Miram Mowat** (Thermap Solutions) for initial TDTR data.

Contacts: zl21970@bristol.ac.uk | dong.liu@bristol.ac.uk

1. Introduction to TRISO fuel particles

Coated fuel particles (commonly “TRISO”) are used in high temperature gas cooled reactors (HTGR). These are typically 1 mm diameter and are packed into graphite or SiC pebbles or pellets. HTGRs enable high thermodynamic efficiency, process heat, and clean hydrogen production.

During operation, various things happen to TRISO particles: (i) kernel swelling, fission products, and gas pressure; (ii) radiation-induced dimensional changes in pyrocarbon and SiC, including creep; (iii) degradation of physical properties from radiation defects

Table 1: Components of a TRISO particle.

Layer	Purpose
Fuel kernel ~500 µm (UO ₂ , UCO, UN)	High assay, low enriched uranium to increase fissile fraction of the particle.
Buffer (porous carbon) ~100 µm thick	Absorbs fission gases. Accommodates dimensional swelling of kernel.
Inner pyrolytic carbon (IPyC) ~40 µm thick	Primary fission product diffusion barrier. Mechanical support.
SiC ~35 µm thick	Structural “pressure vessel”. Prevents oxidation in accidents.
Outer pyrolytic carbon (OPyC) ~40 µm thick	Mechanical support and integration into fuel element.

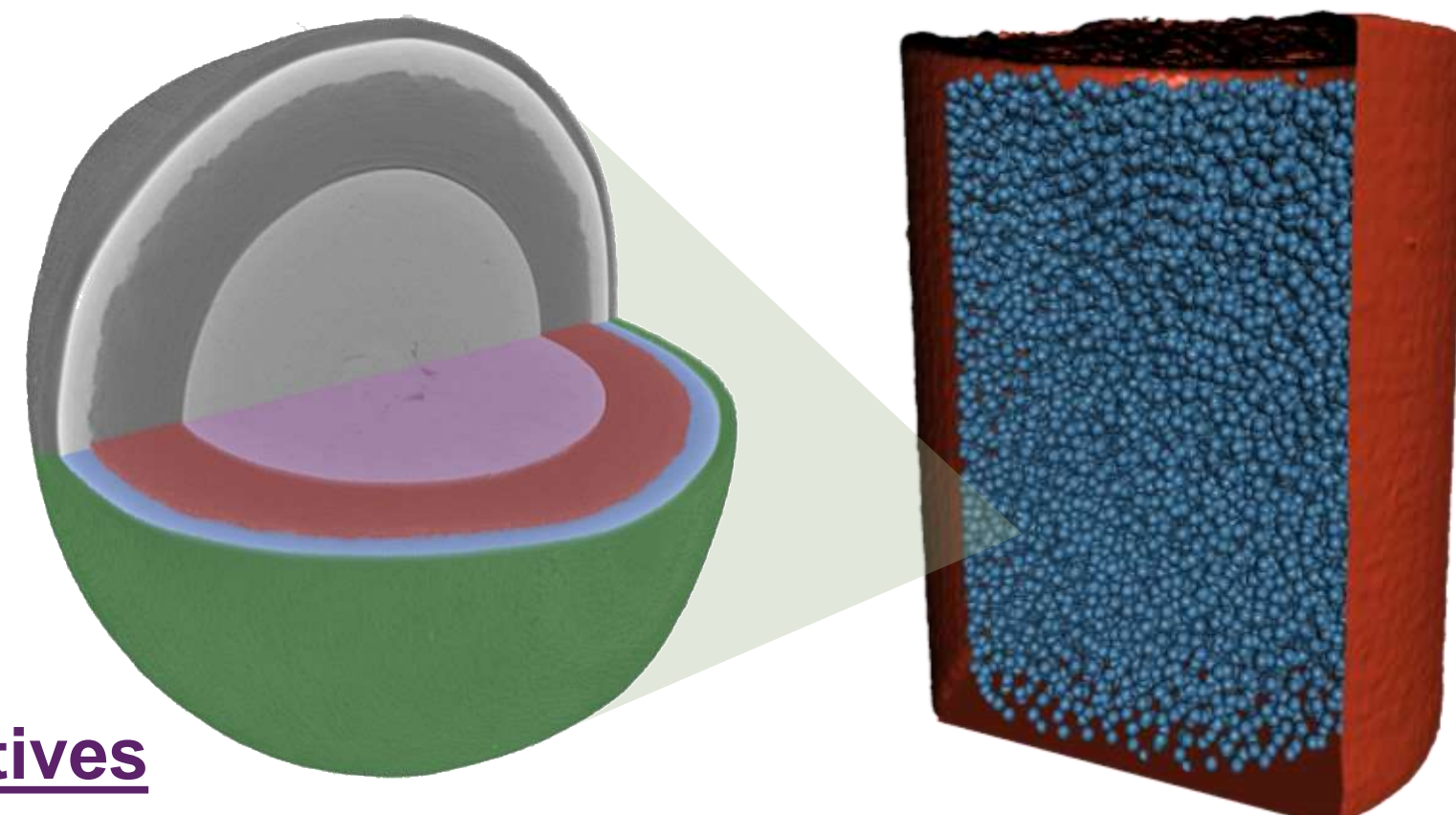


Fig. 1 Segmented X-ray tomography of a coated particle and particles packed into a fuel pellet.

2. Project objectives

We need to experimentally measure the following properties to assist the understanding of the degradation of TRISO particles in service.

- **Micromechanical properties** of each coating and interface
- **Residual stresses** in coatings
- **Dimensional changes**, and radiation creep
- Thermal properties (see adjacent poster)

3. X-ray tomography

- Segmentation achieved by *Dragonfly 2020* using deep learning.
- Mesh generation and 3D mesh thickness calculation.
- **Buffer contracts** with irradiation, and **PyC thickens**.

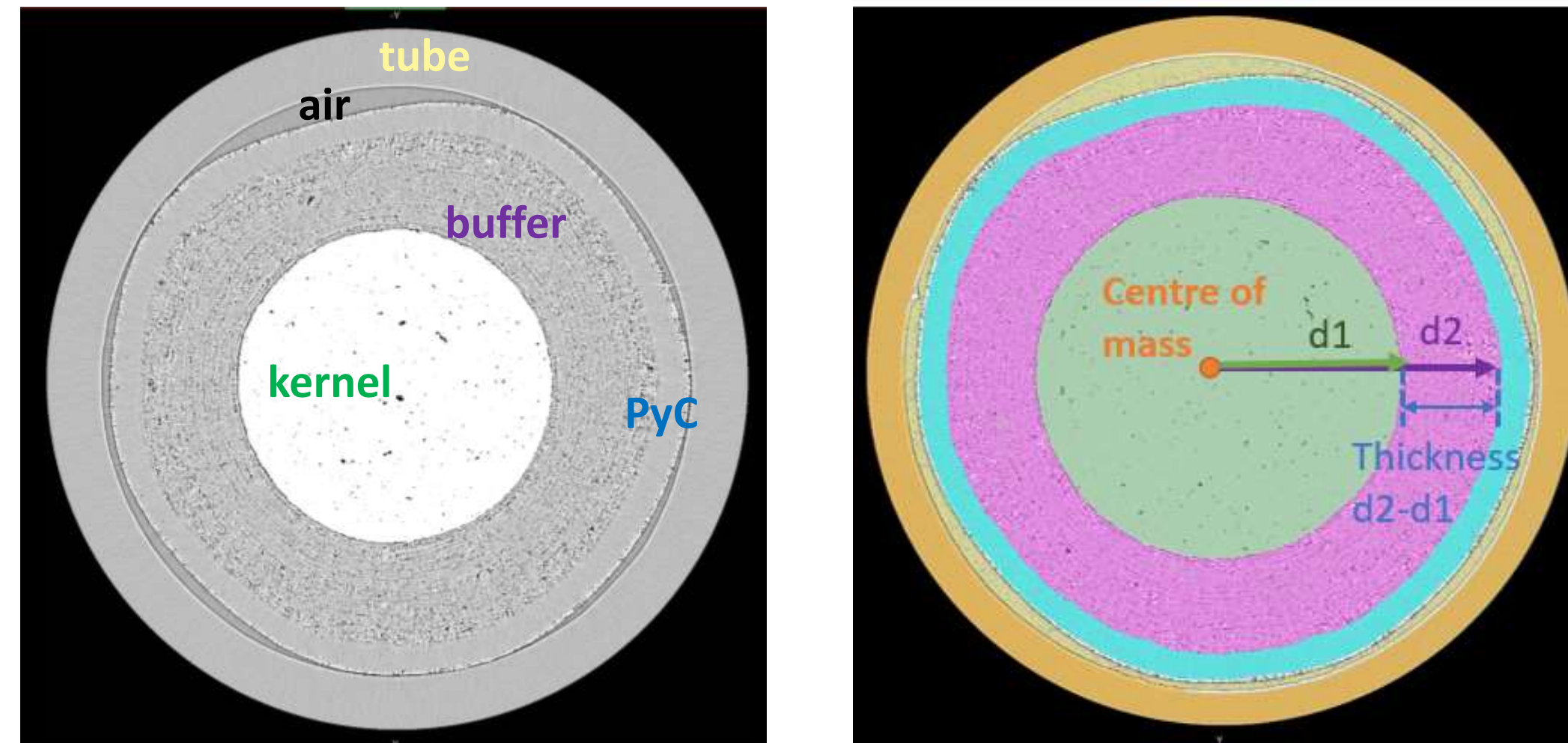


Fig. 2 and Table 2 X-ray tomography and segmentation using deep learning, and 3D thickness measurements made using local thickness meshing.

	This work		Reference [1]		
	High-dose	Low-dose	High-dose	Low-dose	Unirradiated
Buffer	205.0±11.0	225.0±13.0	193.9±10.4	197.4±8.5	225.1±9.4
PyC	70.0±5.0	65.0±7.0	60.4±2.4	61.3±2.1	59.1± 2.1

Unit: µm

4. Microcantilever bending

Test the strength of SiC/IPyC boundaries in surrogate TRISO. Microcantilevers prepared by FIB and broken in nanoindenter.

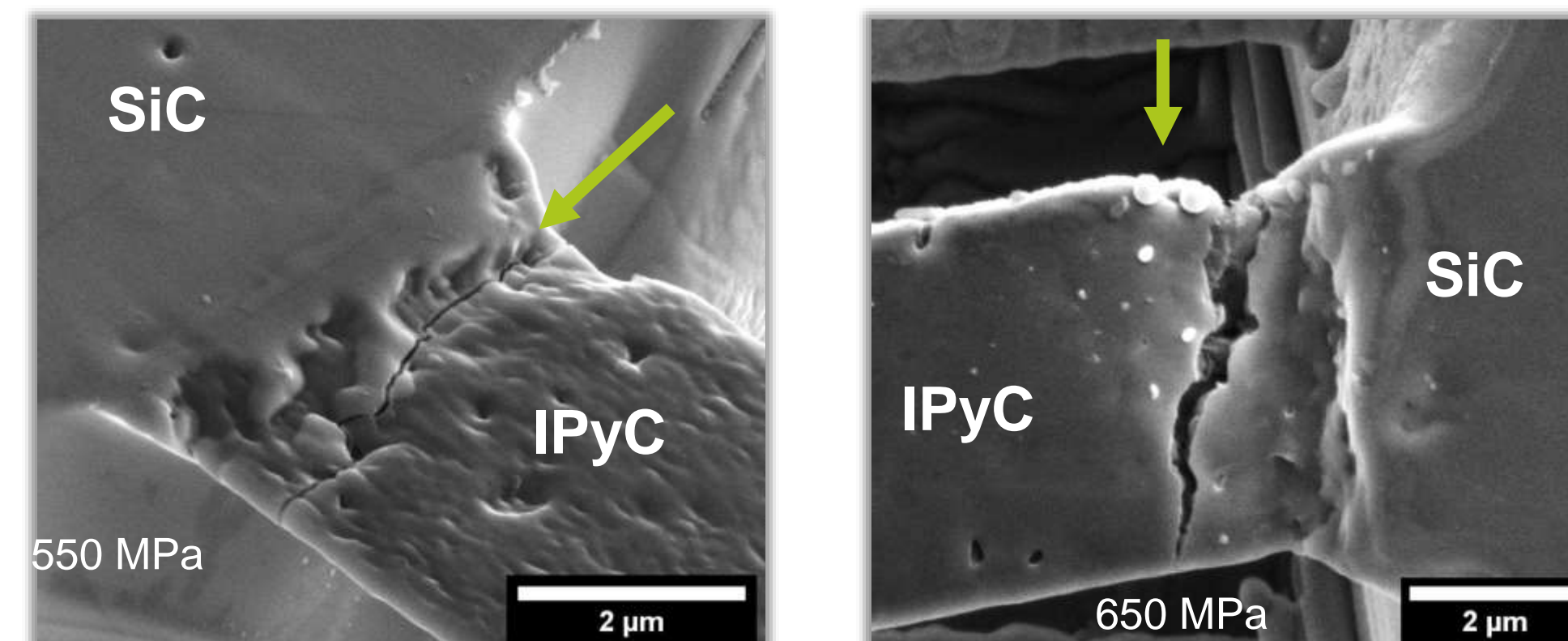


Fig. 3 Failure from pores or percolated SiC in IPyC rather than at the boundary. Strength close to pyrolytic carbon strength [2].

5. FIB-DIC residual stress

1. Incrementally mill a ring to relieve residual stress locally in a coating layer.
2. SEM imaging and DIC analysis to track changes and calculate strain relief.
3. Calculate residual stress from strain relief and elastic constants.

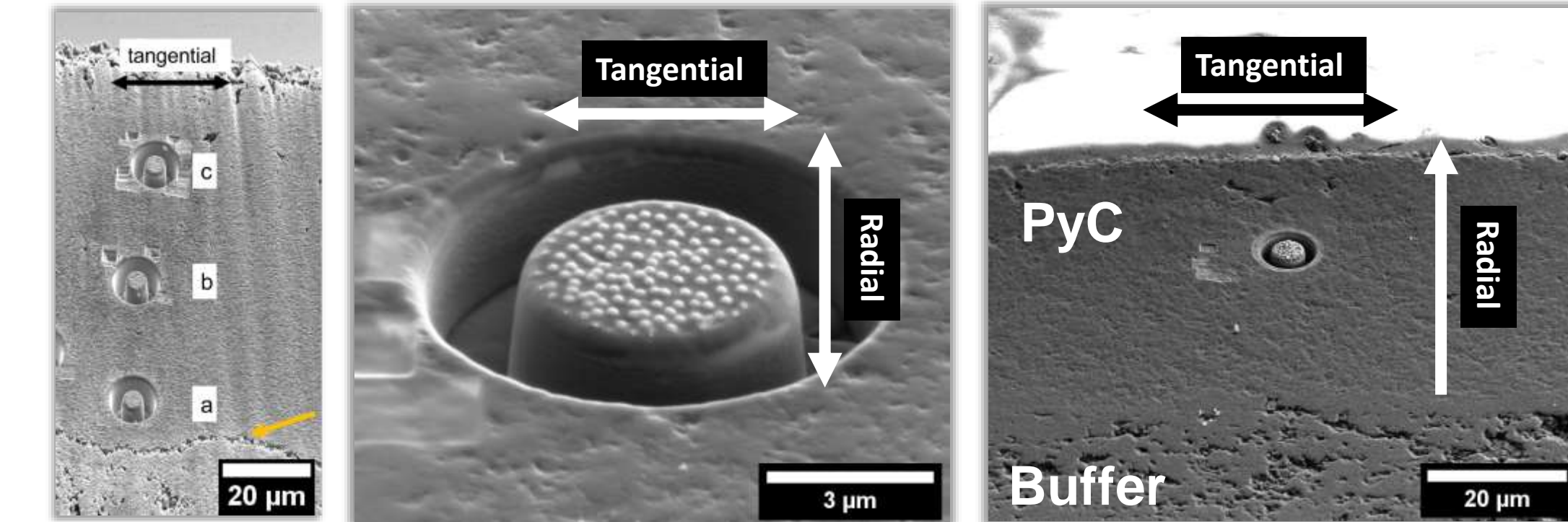


Fig. 4 FIB-DIC measurements of unirradiated and neutron irradiated PYCASSO particles.

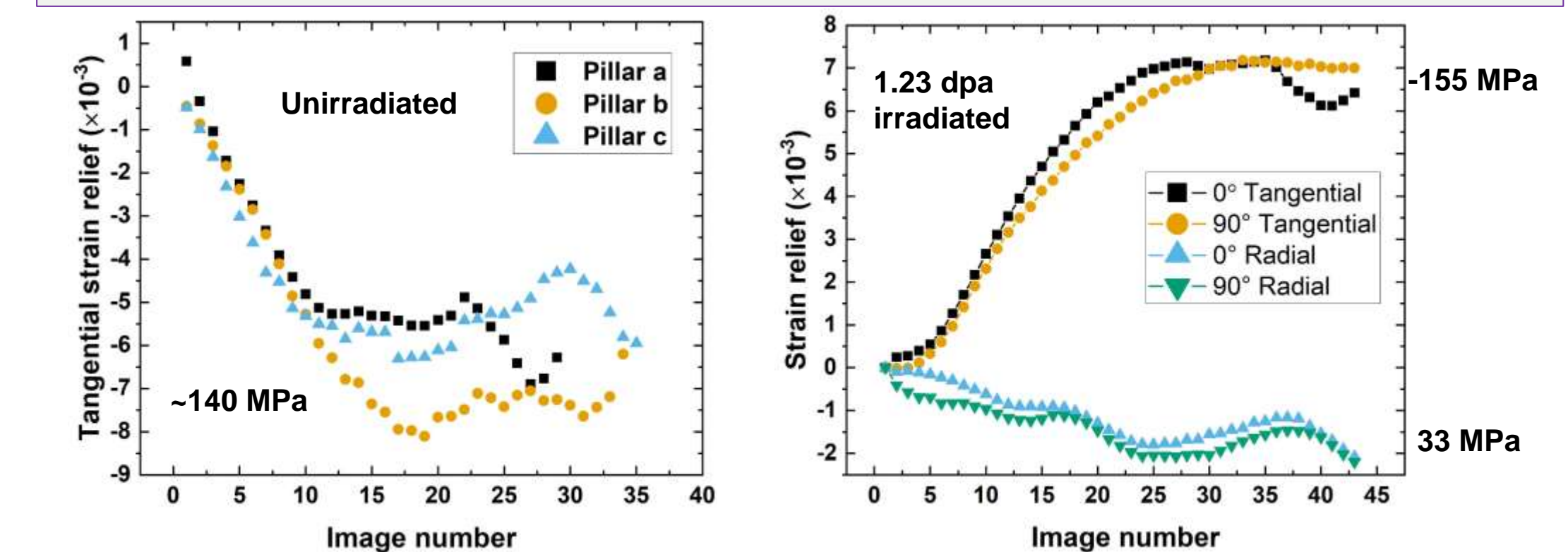


Fig. 5 Strain relief curves for unirradiated and irradiated PyC in PYCASSO particles

6. Conclusions

- Radiation-induced dimensional changes observed by XCT.
- SiC/IPyC interface is stronger than IPyC.
- **Tensile** residual hoop stress in *unirradiated* PyC-1 pyrocarbon
- **Compressive** hoop stress in *irradiated* PyC-1 pyrocarbon caused by radiation-induced dimension changes. Radial stress is much smaller.

7. References, acknowledgements & contact

- [1] Liu, D. *et al.* X-ray tomography study on the crushing strength and irradiation behaviour of dedicated tristructural isotropic nuclear fuel particles at 1000 ° C. *Mater. Des.* **187**, 108382 (2020).
 [2] J.C. Bokros, Carbon biomedical devices, Carbon N. Y. (1977) 353-371.

This work was funded under the £46m Advanced Fuel Cycle Programme as part of the Department for Business, Energy and Industrial Strategy’s (BEIS) £505m Energy Innovation Programme.

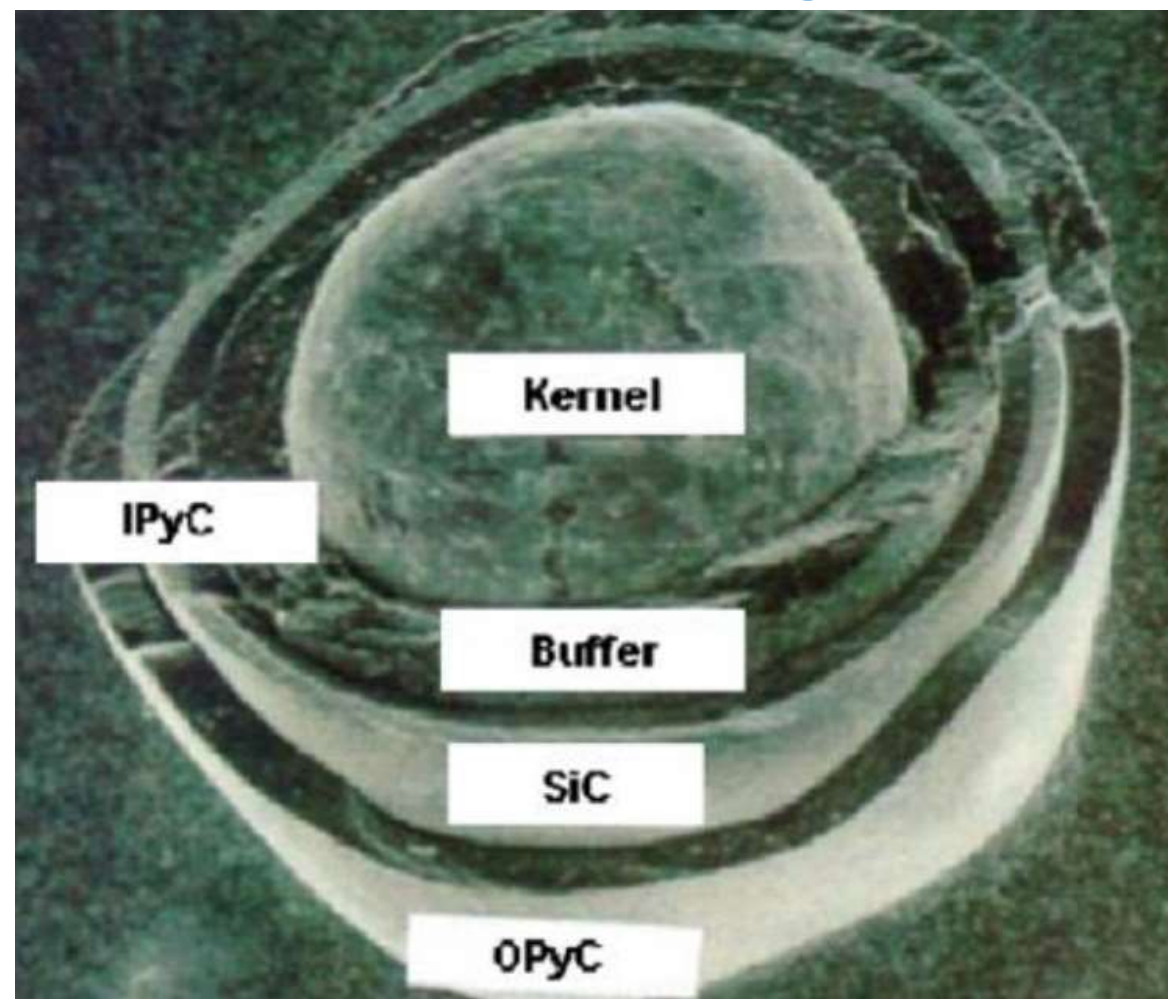
Dr Josh Kane (Idaho National Laboratory) for providing irradiated PYCASSO samples.

Mark Davies (Ultra Safe Nuclear Corporation) for providing surrogate TRISO particles.

yf20941@bristol.ac.uk | alex.leide@bristol.ac.uk | dong.liu@bristol.ac.uk

Introduction and Scope

TRISO Fuel and High Temperature Gas-cooled Reactors



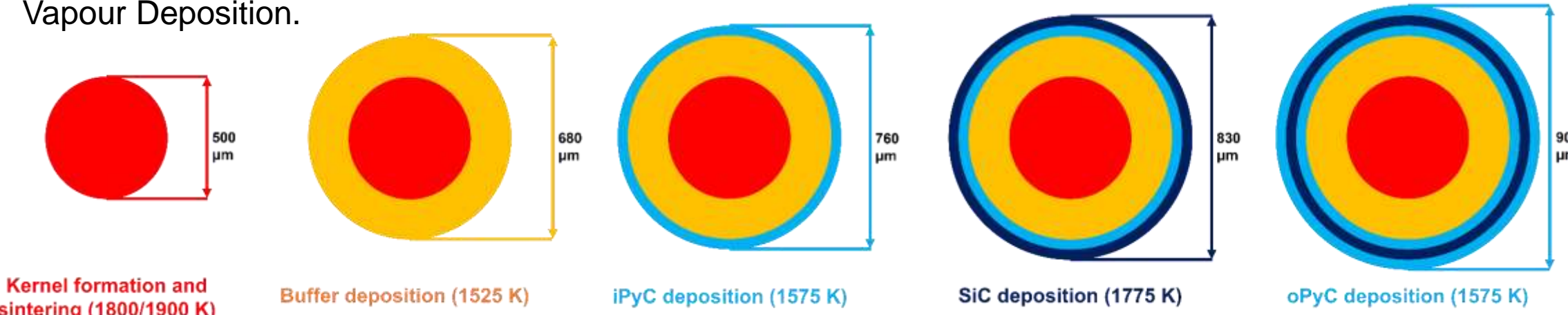
TRistructural ISOtropic (TRISO) coated particle fuel [1] is an advanced technology fuel (ATF) designed to bring the accident tolerance of nuclear energy production to an extreme level. It is composed of a spherical kernel (isotropic), a buffer layer and 3 protective layers (tristructural). It is also the fuel for modern High Temperature Gas-cooled Reactor (HTGRs) which offer the potential to decarbonise hard-to abate energy sectors through the provision of high-temperature process heat for industry or green hydrogen production

The analyses conducted for this project will improve the understanding of the fuel choice for modern HTGRs.

A thorough analysis of the initial stress state of TRISO particles before their adoption in HTGRs is fundamental for the development of accurate performance models for this type of fuel. This is due to several effects, such as the gaseous fission products accumulation in the kernel, which will unavoidably lead to a complex stress profile in TRISO during operation.

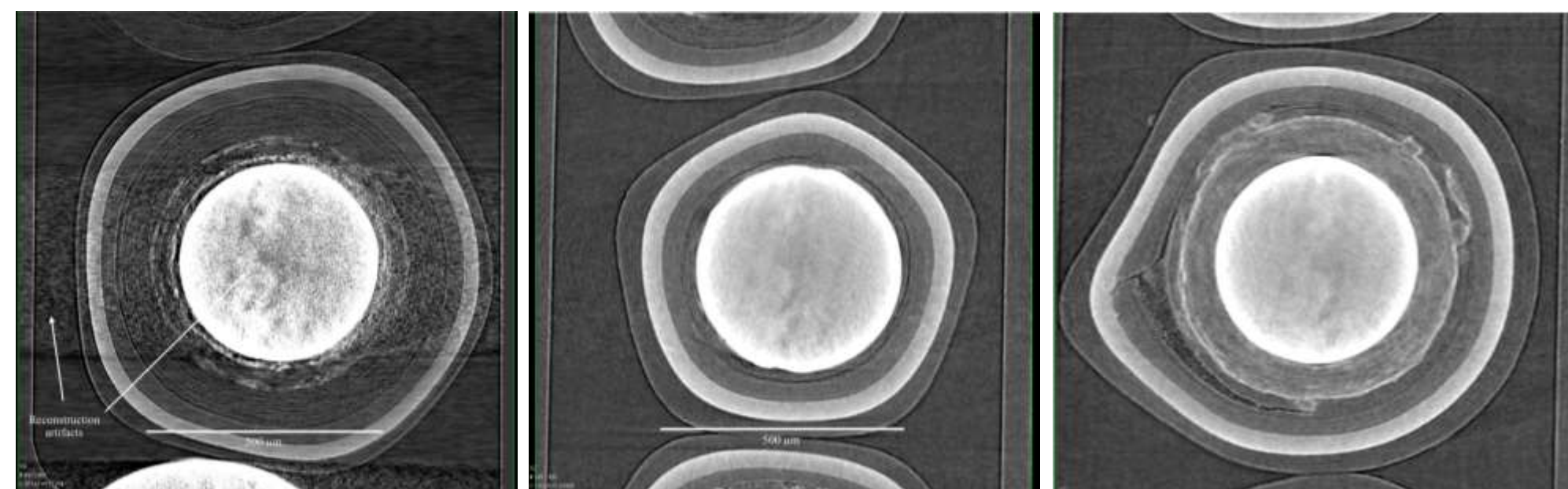
Fabrication of TRISO Fuel

The carbon and ceramic layers of TRISO particles are sequentially built-up by Fluidised Bed Chemical Vapour Deposition.



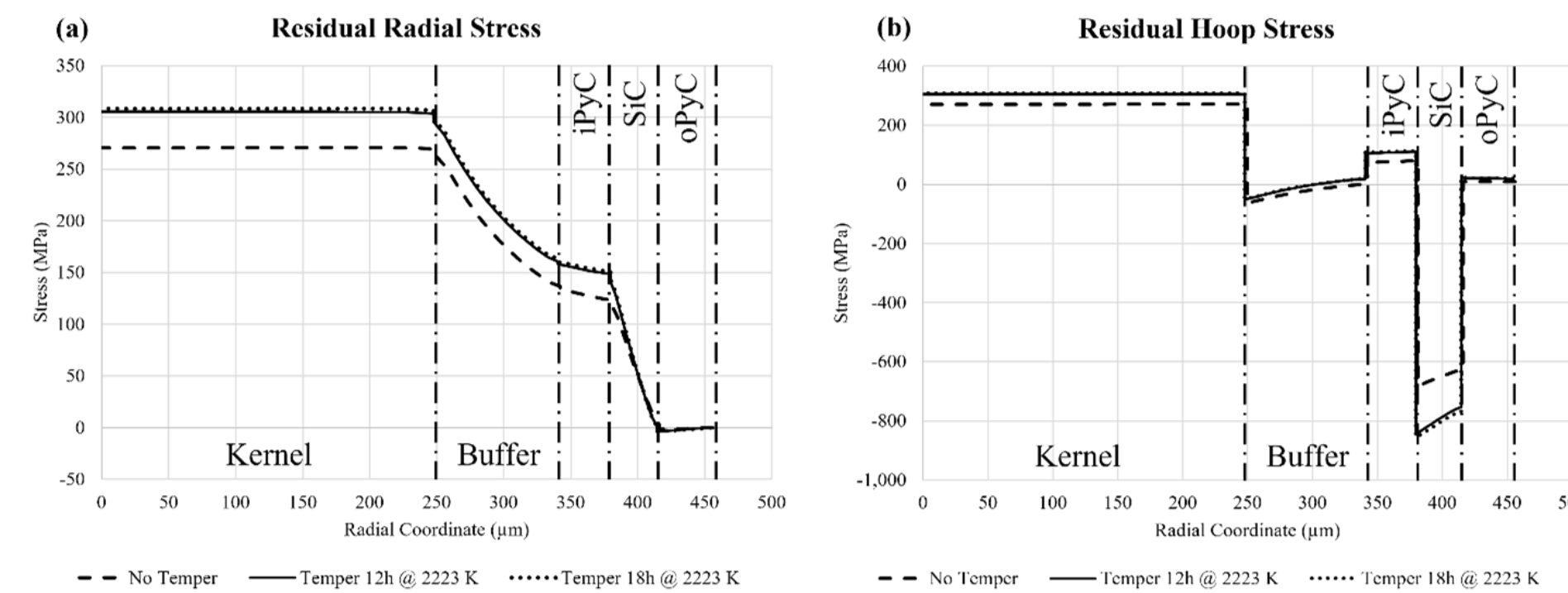
Anomalies in TRISO Particles: Ovality and Layer Decoupling

Due to the high temperatures involved in the fabrication of TRISO and the heterogeneity of the materials adopted [2], the debonding of layers is a possibility. Indeed, if operational stresses are added to ones potentially pre-existing from fabrication (the CVD process itself is prone to the production of shapes with different degrees of ovality, which could affect the distribution of residual stresses), they could lead to the premature failure of the particle or an opportunity for longer fuel life and greater burnups. This is endorsed by several micrographs available in literature [3], where the buffer layer is essentially detached from the kernels after fabrication.

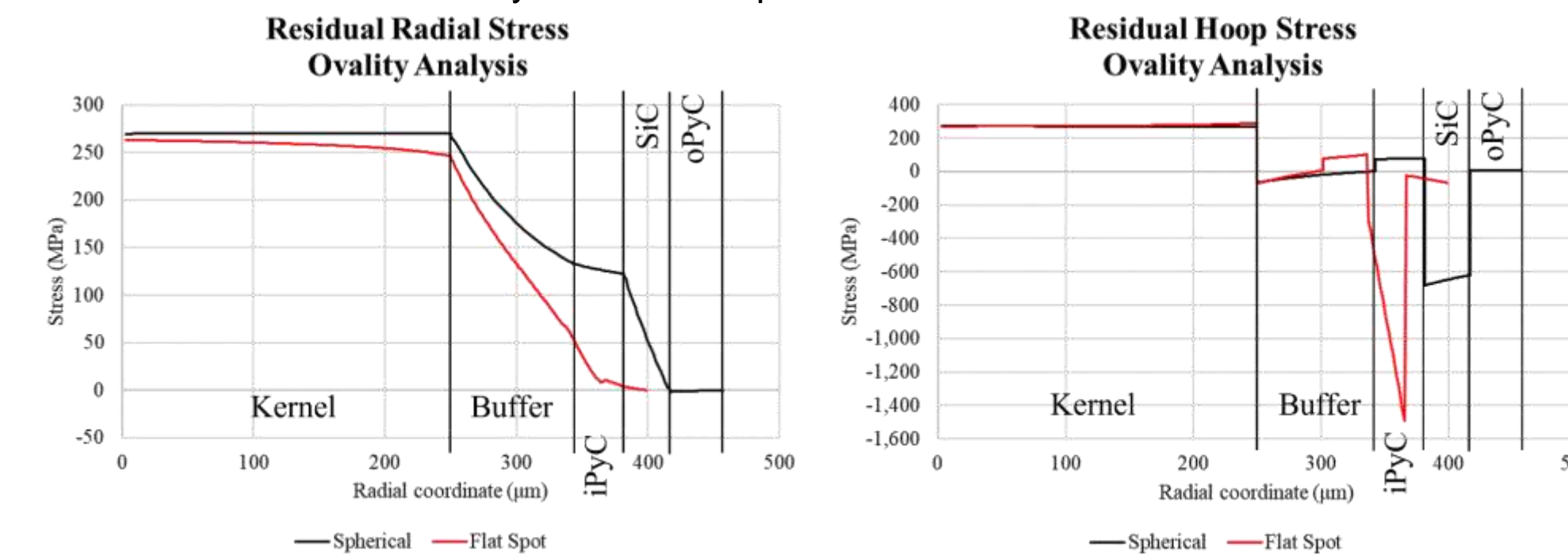


Results

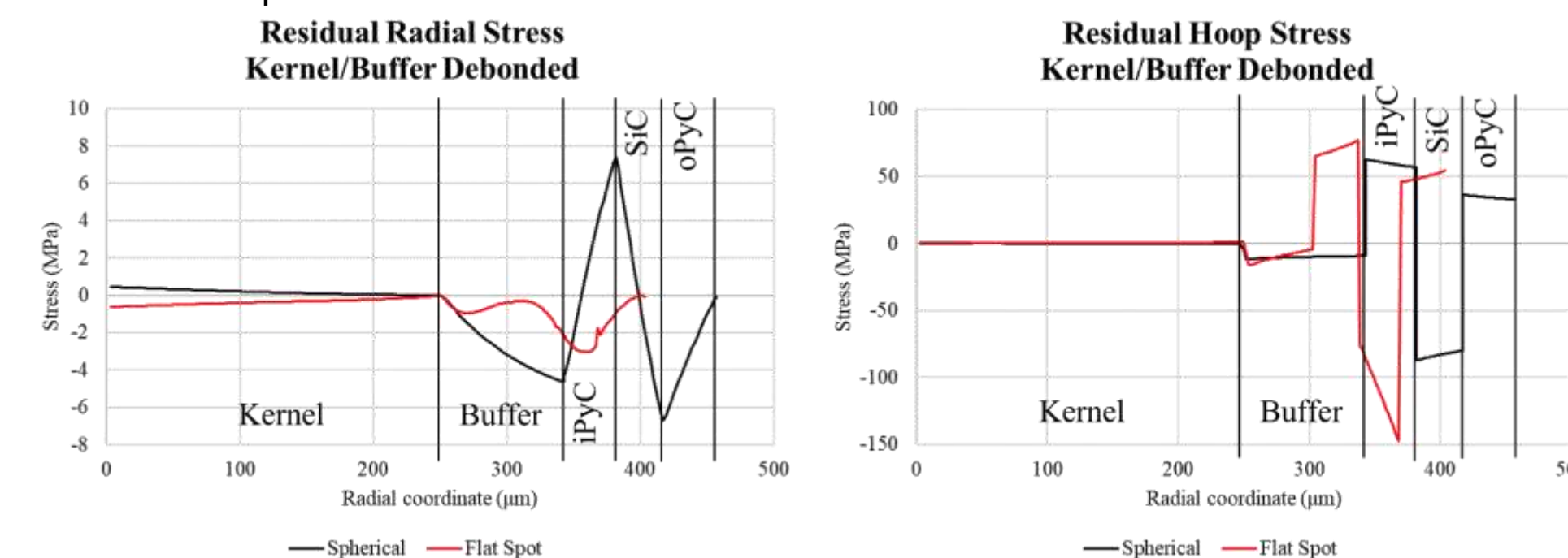
The preliminary results of the fabrication process are based on a fully bonded model, where the 4 layers of the TRISO particle are not allowed to detach from each other. This resulted in great tensile (~200MPa) residual stresses in the kernel (radial and tangential) and buffer (radial). At the same time, a greater value of compressive hoop stress (~600 MPa) is seen in the SiC layer and exacerbated by the tempering phase, most likely due to the smaller expansion coefficient and the greater elastic modulus of SiC.



The ovality study was focused on an extreme situation, where a flat spot caused by a problem in the buffer deposition step is included in the model. The analyses pertaining to this situation show how the residual stress in the flat spot are greater in the hoop direction. This is most evident in the fully coupled model above, whereas the results for the decoupled model confirm the relaxation already seen in the spherical model.

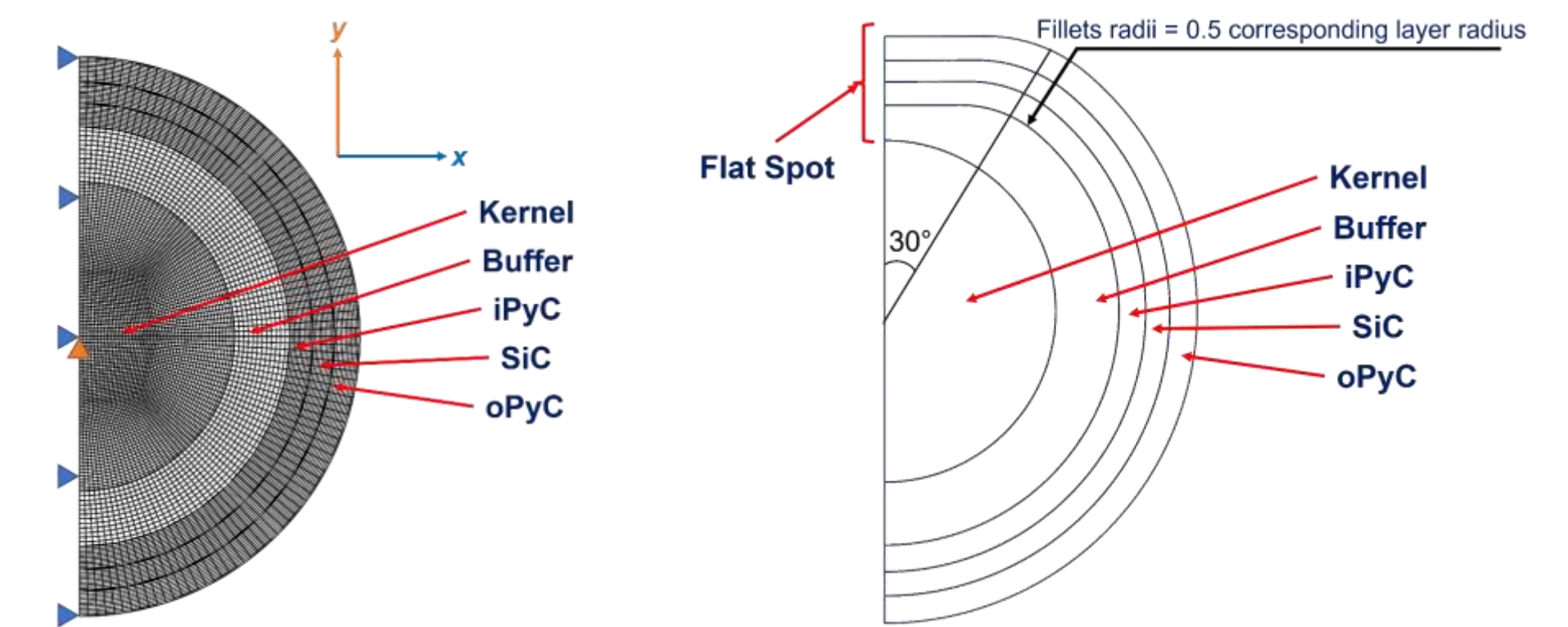


The models featuring a fully decoupled buffer layer from the kernel, however, confirm how such a configuration may help release most of the stresses seen in the preliminary results. In these simulations, the maximum tensile stresses are now observed in the inner PyC layer (~50 MPa hoop), with compression still dominating the SiC layer hoop stress (~100 MPa). The radial stresses, instead, seem to be almost completely relieved, with values in the range of 6 MPa compressive and tensile.



Models

- ABAQUS finite element model
- Axial symmetry
- Material properties extracted from [4]
- Uniform temperature change
- Standard spatial constraints on the particle's axis
- Creep effects modelled for UO₂ and SiC only
- Tempering phase added (hold at 2225 K for 12 and 18 hours)
- Oval models feature a 30° angle flat spot
- Decoupling of layers modelled as hard contact instead of tie constraints



Conclusions

- The manufacture process of TRISO particles may leave some significant residual stresses, which eventually will affect (possibly positively, due to the compressive state of the SiC layer) the behaviour of the fuel during operations.
- The magnitude of the radial stresses retrieved in the kernel-buffer interface hints at the possibility for decohesion of the layers.
- Debonding of the layers releases the stresses in the particle, leading to a more relaxed but also possibly permeable particle.
- Ovality effects can be important in determining the final stress state of the particle, even if the layers have de-bonded.

References

[1] www.energy.gov/ne/articles/triso-particles-most-robust-nuclear-fuel-earth
 [2] D. A. Petti et al., "Key differences in the fabrication, irradiation and high temperature accident testing of US and German TRISO-coated particle fuel, and their implications on fuel performance" Nucl. Eng. Des., **2003**, 222, 2–3, 281–297.
 [3] Oak Ridge National Laboratory - X-ray Analysis of Defects and Anomalies in AGR-5/6/7 TRISO Particles, June 2017 - ORNL/TM-2017/038
 [4] T. A. Haynes, M. R. Wenman, and D. Shepherd, "TRISO Particle Fuel Brief Literature Review Material Properties," 2021, NNL 15434.

Acknowledgements

This work was funded under the £46m Advanced Fuel Cycle Programme as part of the Department for Business, Energy and Industrial Strategy's (BEIS) £505m Energy Innovation Programme.

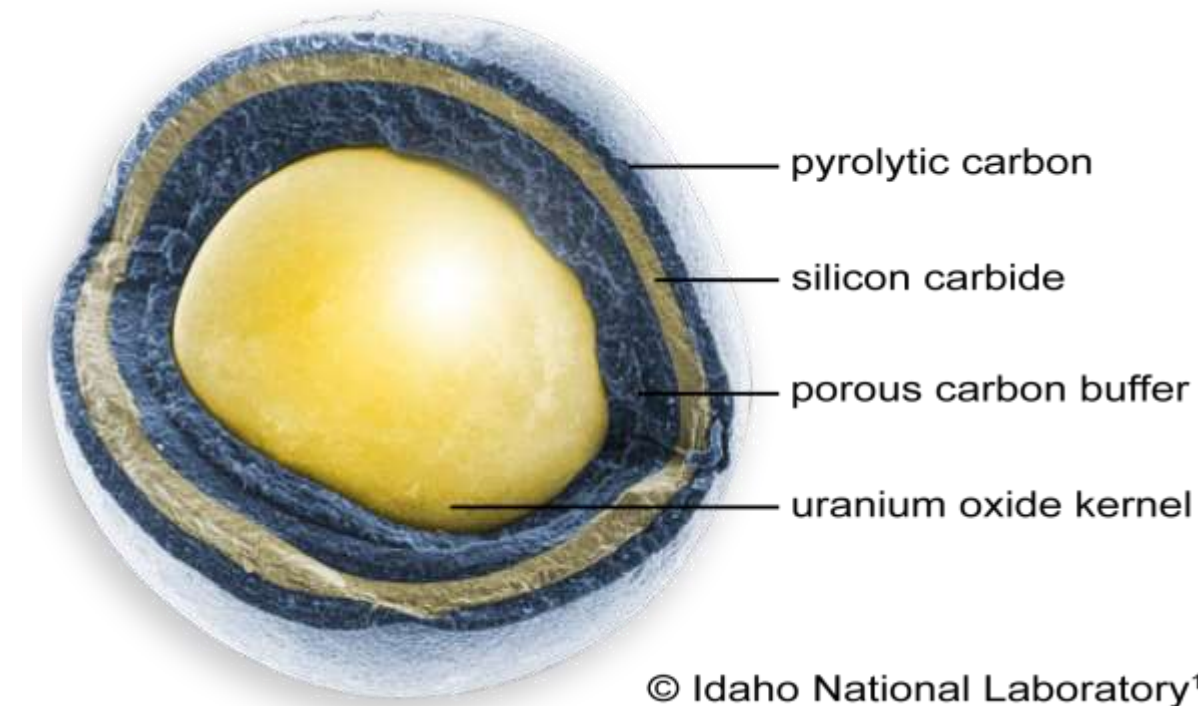
Contacts

Angelo Battistini: a.battistini20@imperial.ac.uk
 Thomas Haynes: t.haynes@uea.ac.uk

Mark Wenman: m.wenman@imperial.ac.uk
 Daniel Shepherd: daniel.shepherd@uknnl.com

INTRODUCTION

Key research within the Advanced Fuel Cycle Programme (AFCP) includes fabrication routes for advanced nuclear fuels, including Coated Particle Fuels (CPF) for use in modern High Temperature Gas-cooled Reactor designs. To enable study of the optimal conditions for the generation of spherical ammonium diuranate (ADU), a key precursor to UO_2 kernels, a new lab-scale kernel production and testing facility has been established at Lancaster University.



© Idaho National Laboratory¹

OBJECTIVES

- Establish UO_2 kernel manufacturing capability within a non-industrial setting using the established chemical gelation route.
- Understanding of chemical gelation process – a rapid reaction of uranium & ammonia to form ammonium diuranate (ADU).
- Fabricate UO_2 kernels within target parameters²⁻⁴ & generate kernel material for subsequent coating with carbon / ceramic layers to give CPF.

EXPERIMENTAL METHODS

CASTING:

- Uranium casting solution distributed from nib – uranyl nitrate hexahydrate (120 g/l U)
- Surface tension modifiers ensure spherical droplet morphology – THFA & PVA
- Ammonia gas curtain – initiates gelation & fixes droplet shape in place

AGEING:

- Ammonium hydroxide ageing solution – reacts with uranium to form ADU throughout kernel
- In-column – 7 M @ 25°C for 5 min; continued ageing – 3 M @ 80°C for 60 min

WASH & DRYING:

- 3 x water & 1 x isopropanol wash cycles to remove by-products
- Air dry @ 30°C for 60 min, oven dry @ 80°C for 3 hours

CALCINATION:

- Dried kernels heated to 430°C in air – 19.3% mass & 20.1% diameter reduction
- Removal of residual water, decomposes polymeric agents, converts ADU to UO_3

REDUCTION & SINTERING:

- Kernels heated to 750°C in reductive atmosphere (2.5% H_2) – reduce UO_3 to UO_2
- Kernels heated to 1600°C in a reductive atmosphere (2.5% H_2) to produce a dense ceramic

ANALYSIS:

- Thermogravimetric analysis & Raman spectroscopy – Stoichiometry (U:O ratio)
- Scanning electron & laser scanning microscopy – morphology and sphericity measurement
- Energy-dispersive X-ray spectroscopy – impurity content

RESULTS

Within a short period of time, a CPF manufacturing rig has been designed, commissioned and successfully deployed for the manufacture of spherical ADU kernels via the chemical gelation route. ADU kernels have been successfully converted to UO_3 and initial analysis performed.



Various casting nib morphologies and sizes have been investigated with the latter having a direct effect on kernel diameter. To date, kernels have been manufactured to a consistent particle diameter of 775 μm after calcination.

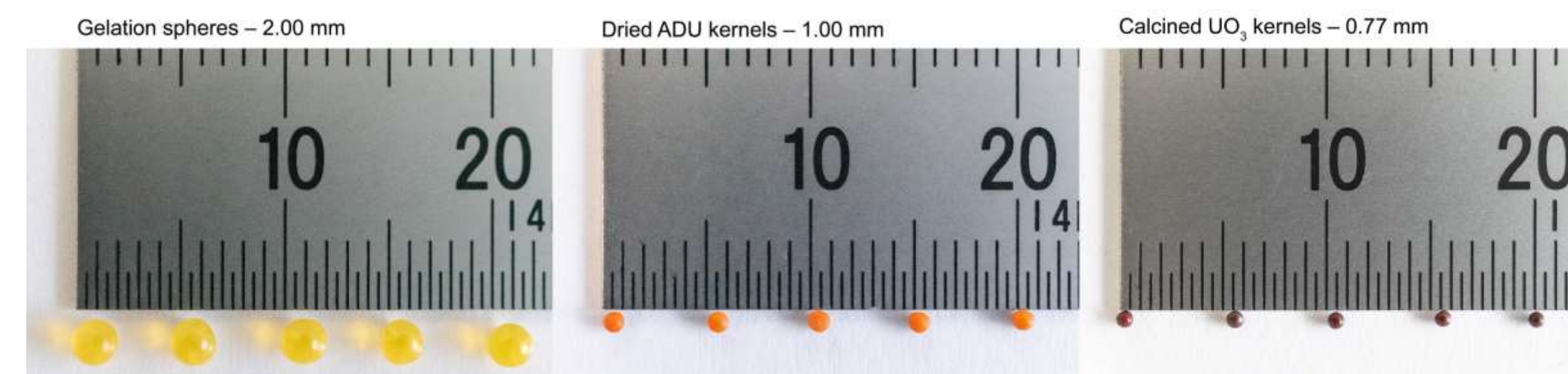
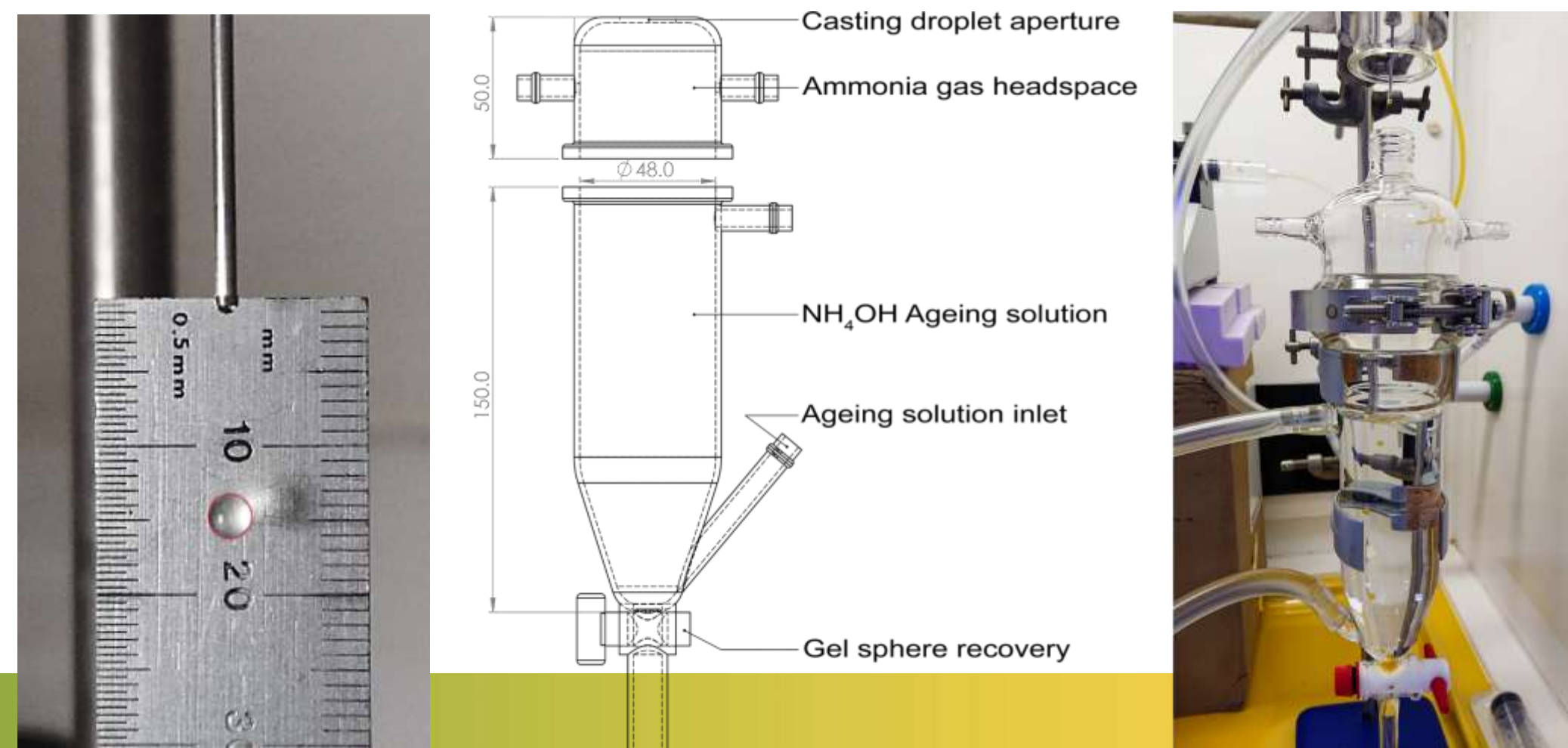
The deployment of an ammonia gas curtain within the casting column significantly enhances the sphericity of cast-kernels via formation of a pre-hardened shell prior to impact with the ageing solution. Absence of this pre-hardening stage results in kernel deformation, see below.

ONGOING & FUTURE WORK

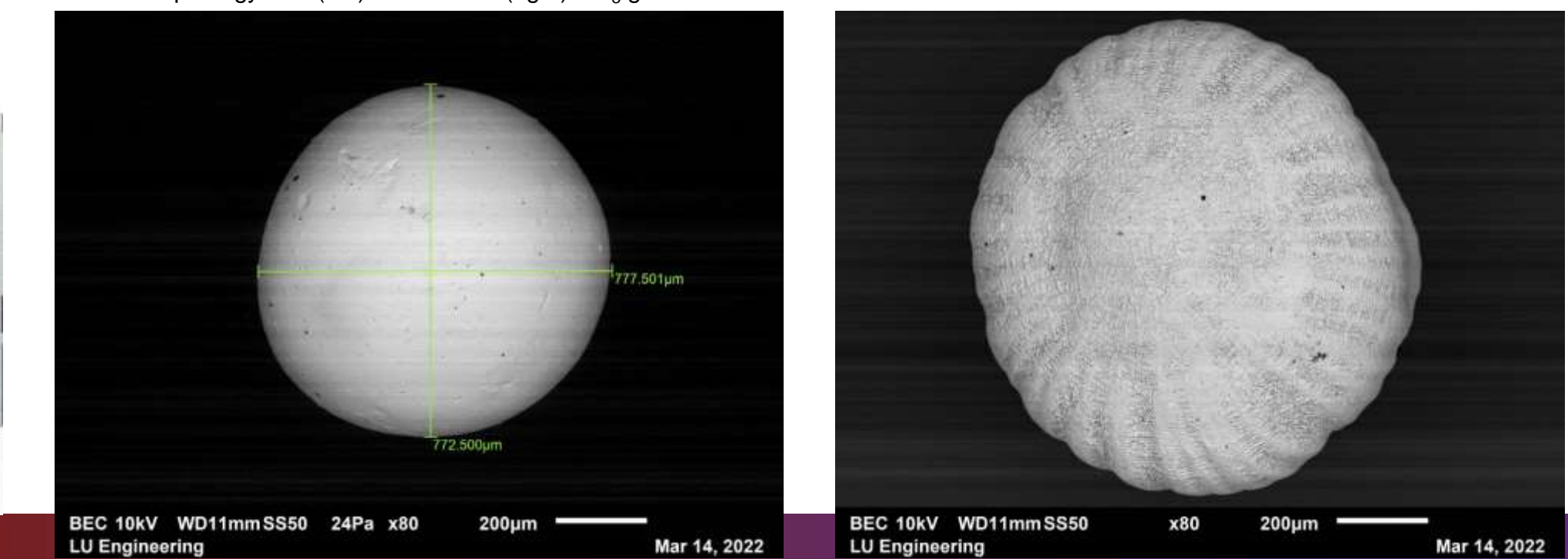
Further optimisation of casting rig parameters:

- Casting solution flow rate and temperature
- Nib vibration system to aid droplet detachment

Continued analysis of fabricated kernels & reduction to UO_2
Comparison of “internal” vs “external” gelation processes



Kernel morphology with (left) and without (right) NH_3 gas curtain



REFERENCES

1. Demkowicz, P.A., B. Liu, and J.D. Hunn, *Coated particle fuel: Historical perspectives and current progress. Journal of Nuclear Materials*, 2019. 515: p. 434-450.
2. Price, M.S.T., *The Dragon Project origins, achievements and legacies. Nuclear Engineering and Design*, 2012. 251: p. 60-68.
3. *High Temperature Gas Cooled Reactor Fuels and Materials. 2010, Vienna: INTERNATIONAL ATOMIC ENERGY AGENCY*
4. Knüfer, H., *Preliminary operating experiences with the AVR at an average hot-gas temperature of 950°C. Nuclear Engineering and Design*, 1975. 34(1): p. 73-83.

ACKNOWLEDGMENTS

This work was funded under the £46m Advanced Fuel Cycle Programme as part of the Department for Business, Energy and Industrial Strategy's (BEIS) £505m Energy Innovation Programme and was carried out at the Lancaster University UTGARD Lab (Uranium / Thorium beta-Gamma Active R&D Lab) – a National Nuclear User Facility supported by the UK Engineering & Physical Sciences Research Council (EPSRC).

INTRODUCTION

A key feature of the Advanced Fuel Cycle Programme is the development of innovative routes to manufacturing advanced nuclear fuels. One novel production route is Flash sintering (FS), where an electric field is applied to a free-standing body either by physically contacting electrodes Fig.1, or contactless electrode head (CFS), Fig. 4 & 5. This offers potential benefits of:

- 50% reduction in sintering time: productivity increase
- Energy efficiency: de-carbonisation
- Significant reduction of furnace temperature (25-50%)
- High processing speeds (Reduction in volatilisation of ions)

As part of the AFCP Phase 2 Fast Reactor Fuels project, also involving NNL and UoM [1], Lucideon demonstrated that contact FS using Lucideon's proprietary control system can be used to manufacture nuclear fuel using surrogates, Fig.2. The outcome of the work was then applied to uranium oxide (UO₂) to produce the first flash sintered UO₂ pellet in the UK.



Fig 2. Evolution of CeO₂ pellets under evolving FS parameters. From left to right, localised melting to homogeneous sintering using applied AC electric fields.

The potential benefits of contactless over contact Flash Sintering;

- It can eliminate the need for intimate electrical contact requirements.
- The rastering mode of CFS can theoretically sinter many samples at once.

OBJECTIVES

The **key objectives** of the project were:

- Find a production route to **manufacture green surrogate kernels** of ~ 1 mm in diameter.
- Assess the **feasibility of contactless flash sintering** in sintering the surrogate green kernels.
 - Via a rastering mode (moving over an array of loosely packed pan granulated spheres).
- Assess the **power dissipation of contactless flash sintering** on a single sample.
 - Via a stationary mode (holding over a single pressed cylindrical pellet).
- Perform a **theoretical analysis and assessment of potential scalable approaches** to sinter kernels.
 - Covering conventional and field assisted methods & identify the most promising approaches.

MATERIALS AND METHODS

The contactless flash sintering system is shown in Fig 3. For rastering experiments the spheres were loaded onto a SiC plate as shown in Fig 4. For stationary experiments pressed cylindrical samples were loaded into short holes drilled into the SiC plate, Fig 5.



Fig 3. The image of contactless FS furnace including robot and control system

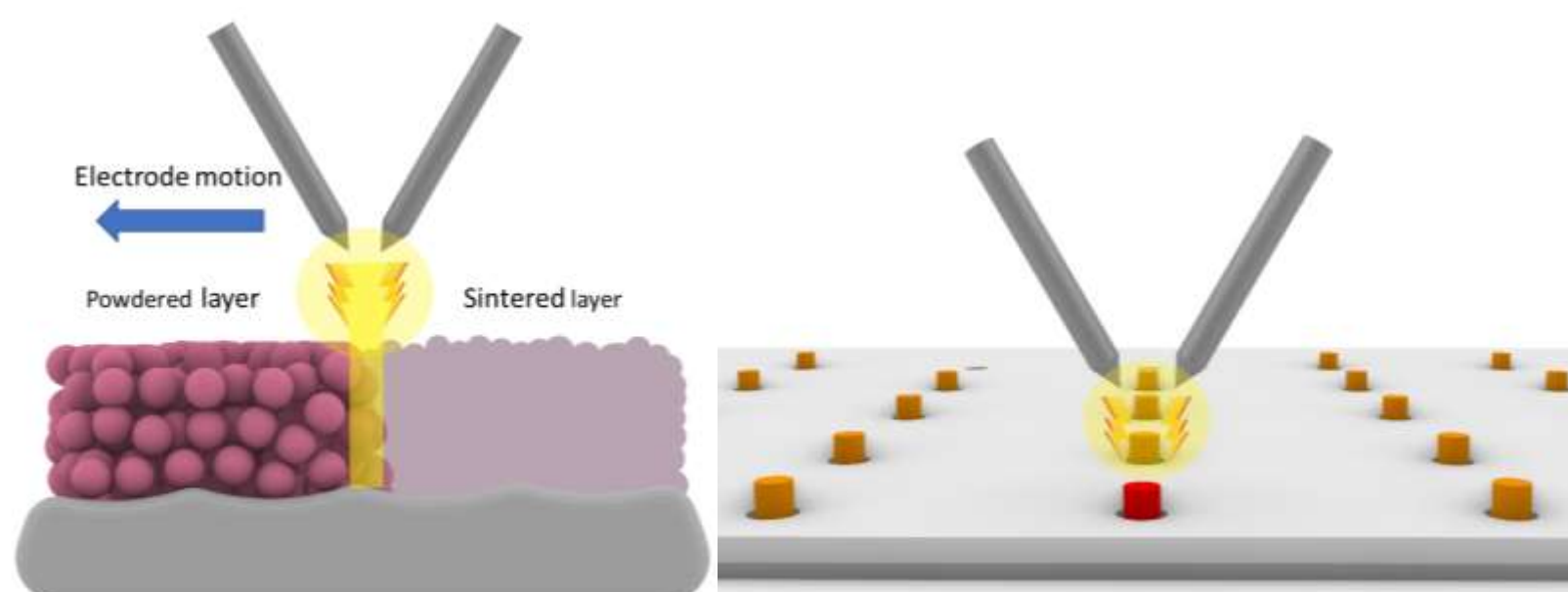


Fig 4. Schematic of rastering contactless FS

Fig 5. Schematic of stationary contactless FS

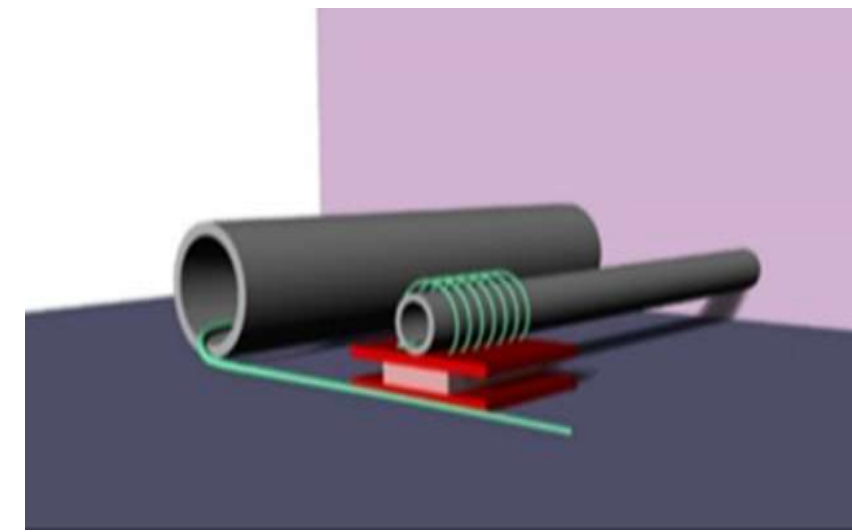


Fig 1. Schematic of contact FS. The pellet sandwiched between two electrodes within the furnace.

RESULTS

Contactless Flash Sintering – Rastering

- Contact FS established 1100-1150°C as a key furnace temperature for CeO₂, and this is consistent for contactless.
- The spark tended to localise and anchor to specific spheres and their immediate neighbours, displaying potential hot-spot formation [2].
- The resulting microstructure is highly varied, with some evidence of melting. Fig 6.

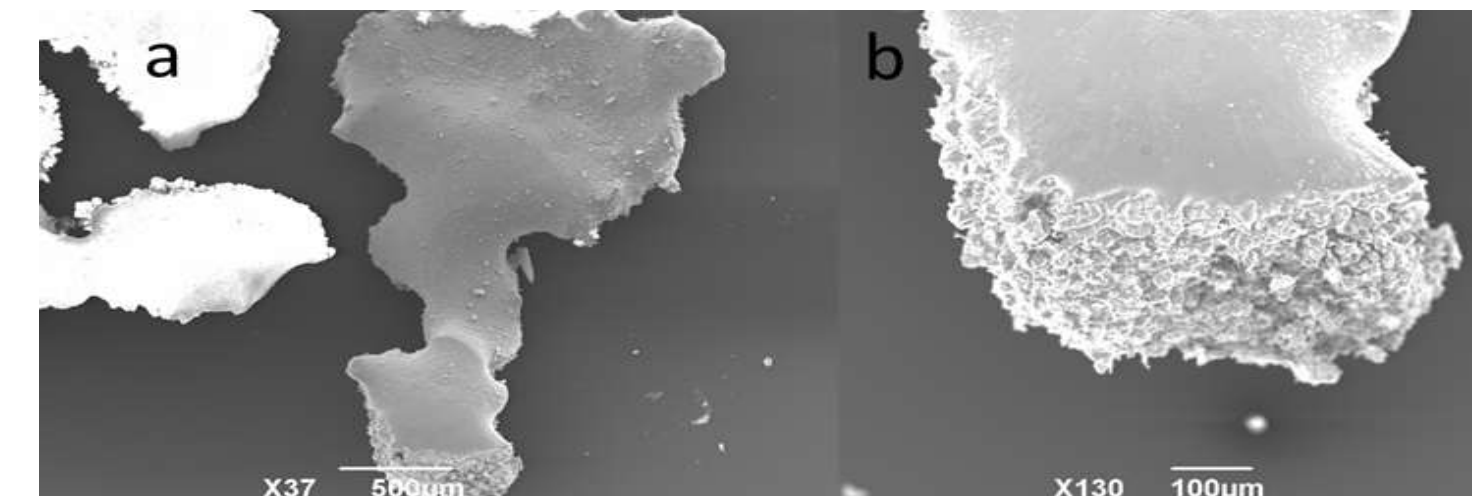


Fig 6. SEM of spheres after rastering CFS at 1100°C a) Multiple spheres bonded together. b) Top melted surface of sample, with more conventional sintered grain structure in cross section.

Contactless Flash Sintering – Stationary

- Masking the supporting electrode material was found to be necessary to prevent the spark straying away from the sample.
- The masking material also acts as thermal insulation, increasing the amount of energy directly dissipated in sample vicinity, allowing reduction of the current and process duration.
- Spark anchors to highly localised points on sample surface causing ablation and melt formation, Fig 7.
- Loading of sample in SiC hole may cause current to bypass bottom of sample, enhancing thermal gradients across the sample.

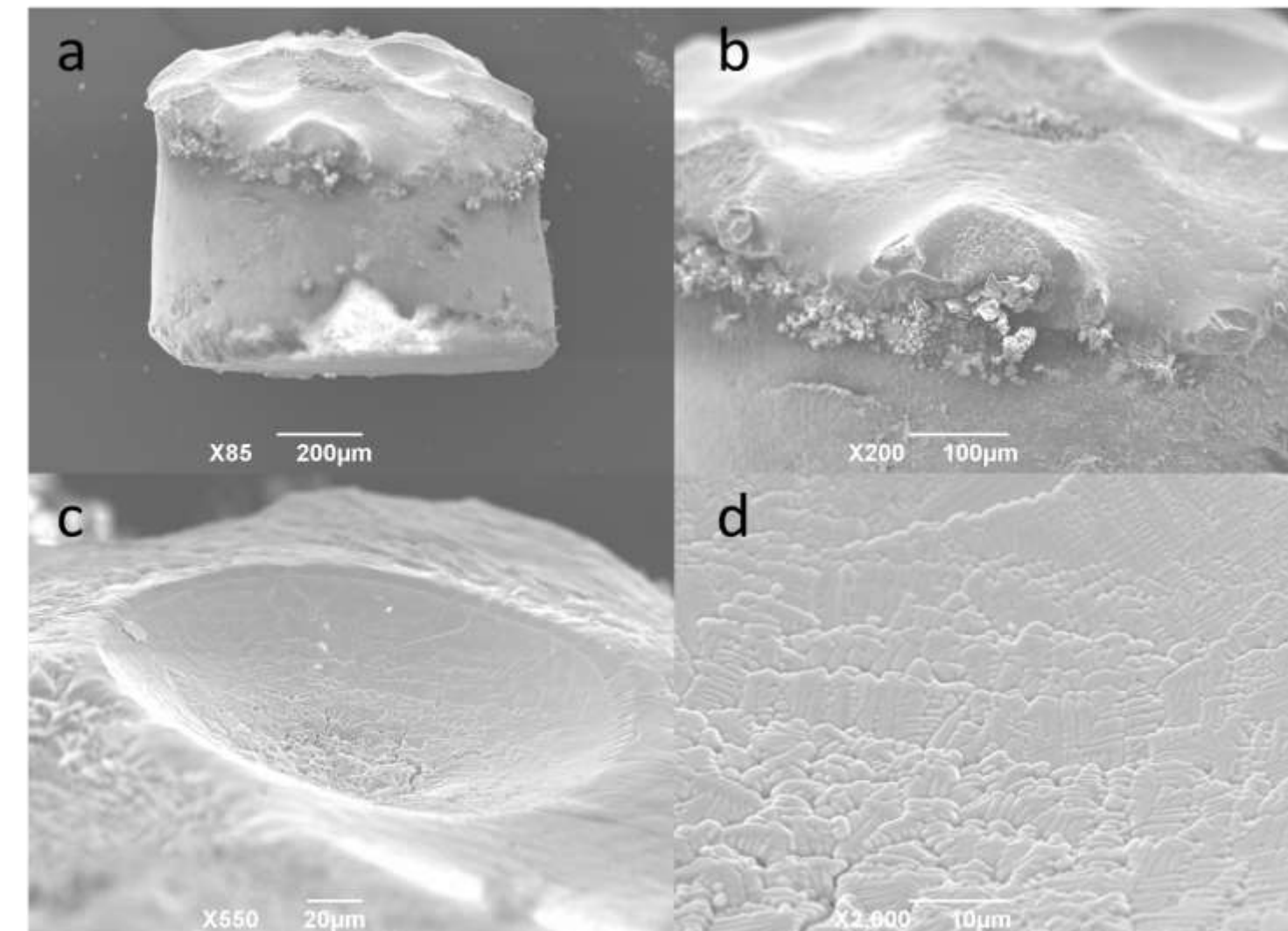


Fig 7. SEM of cylinder after stationary CFS duration 30 seconds at 1000°C. a) Localised effects to top of sample. b) Evidence of multiple arc contacts at top surface. c) Ablated crater from brief arc anchoring. d) Fine microstructure from rapid recrystallisation from melt.

Optimising the Contactless Flash system for TRISO Fuel

- Approaches to be trialed to control hot spot formation:
 - Low frequency electric fields with multiple contactless plasma discharges.
 - Glow discharges.
- Each approach was assessed with respect to: sample shrinkage, possible inhomogeneities and scalability.
- A multi-phase discharge with a Lucideon developed adaptive algorithm was found to be the solution with the most potential due to its ability in homogenizing the current density over the sample i.e. homogeneous sintering.
- A hollow cathode discharge was also found to have potential as glow discharges avoid arc anchoring.

ACKNOWLEDGMENTS

This research was funded under the £46m Advanced Fuel Cycle Programme as part of the Department for Business, Energy and Industrial Strategy's (BEIS) £505m Energy Innovation Programme

Author contact information: Samira.Bostanchi@lucideon.com

CONCLUSION

- Surrogate green kernels were produced by both pan granulation and die pressing methods.
- Trialing of a **rastering contactless flash sintering** had a strong incidence of hot-spots due to the relatively poor electrical and thermal conduction of CeO₂.
 - Improvements may be possible with UO₂, higher furnace temperatures, or better sphere packing.
- Large amounts of energy can be dissipated in the sample during **stationary contactless flash sintering**.
 - However, the thermal dissipation is uneven with ablation and melting of top sample layers.
 - Plasma arc anchors to microscopic points on the sample surface.
- This simple CFS methodology shows limitations in terms of its power dissipation within the sphere samples. **Alternative methods are proposed to harness the rapid nature of CFS but homogenize the power dissipation to the spheres.**
- The challenge of arc localization could be solved by deployment of a **plasma modulation algorithm**, Fig 8.

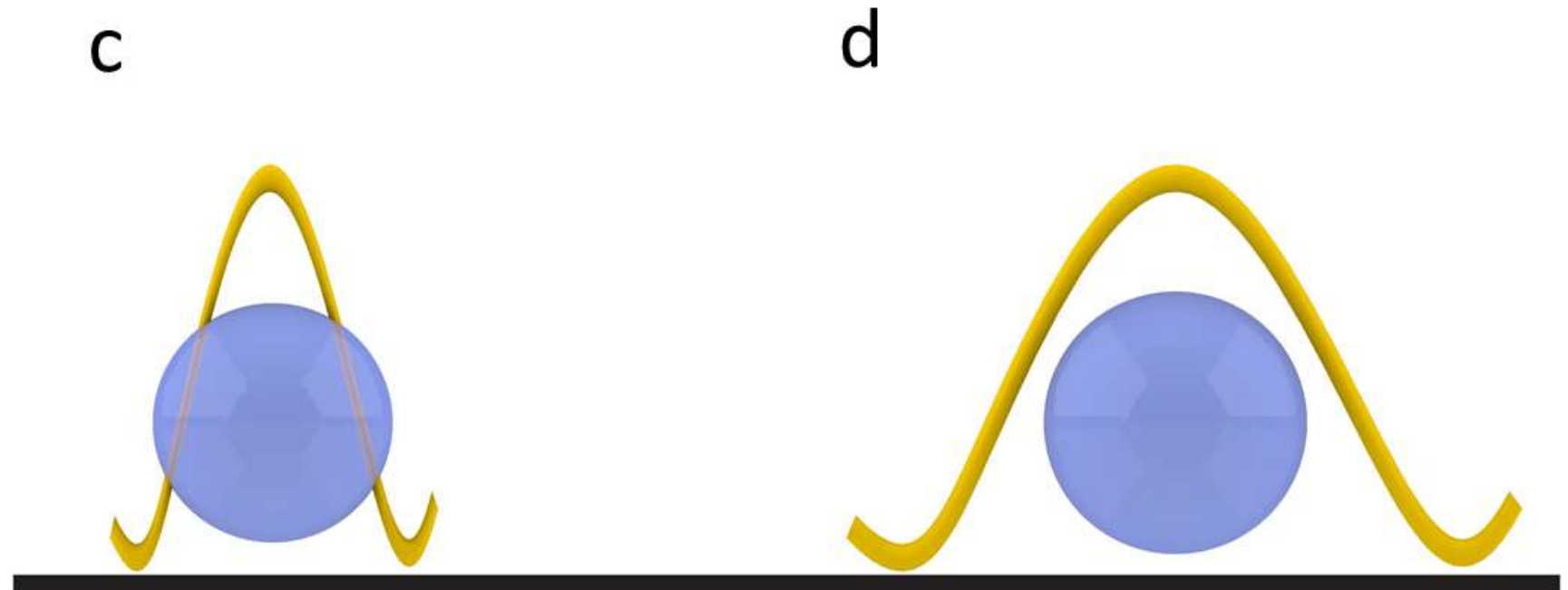
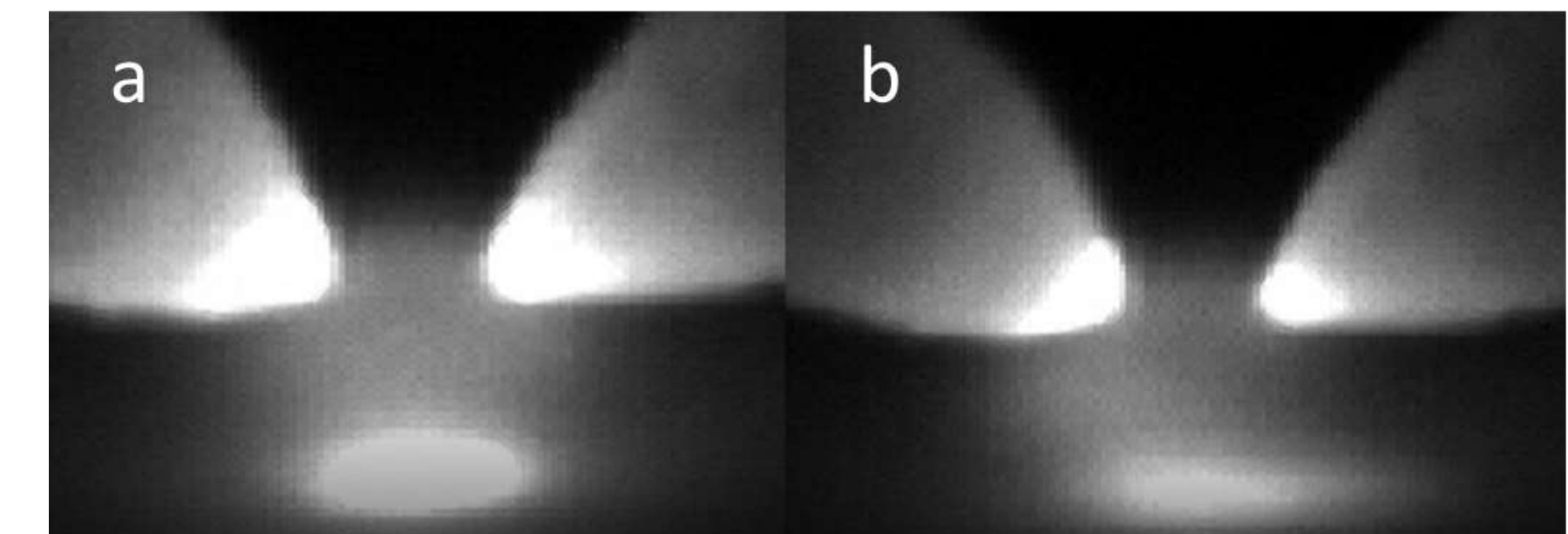


Fig 8. Lucideon plasma modulation algorithm with (a) sharp and (b) diffuse power dissipation settings. (c) schematic of sharp power dissipation shown in (a), and (d) schematic of diffuse power dissipation shown in (b).

- Further work is required to practically test these approaches using:
 - Lucideon's newly developed algorithm suitable for plasma modulation.
 - More conductive surrogate materials.

REFERENCES

- 1) S. Bostanchi, Flash Sintering Feasibility Demonstration on CeO₂, 2021.
- 2) G.M. Jones, M. Biesuz, W. Ji, S.F. John, C. Grimley, C. Manière, C.E.J. Dancer, Promoting microstructural homogeneity during flash sintering of ceramics through thermal management, MRS Bull. 46 (2021) 59–66.